Postprint of: Saddique Z., Imran M., Javaid A., Kanwal F., Latif S., Santos J. E. L., Kim T. H., Boczkaj G., Bismuth-based nanomaterials-assisted photocatalytic water splitting for sustainable hydrogen production, INTERNATIONAL JOURNAL OF HYDROGEN ENERGY (2023), DOI: 10.1016/j.ijhydene.2023.05.047

Bismuth-based nanomaterials-assisted photocatalytic water splitting for sustainable hydrogen production

Zohaib Saddique [a], Muhammad Imran [a,], Ayesha Javaid [a], Farah Kanwal [b], Shoomaila Latif [c], José Cleiton Sousa dos Santos [d,e], Tak H. Kim [f], Grzegorz Boczkaj [g,h,**]*

[a] *Centre for Inorganic Chemistry, School of Chemistry, University of the Punjab Lahore, 54000, Pakistan*
[b] *Centre for Physical Chemistry, School of Chemistry, University of the Punjab Lahore, 54000, Pakistan*
[c] *School of Physical Sciences, University of the Punjab, Lahore, 54000, Pakistan*
[d] *Departamento de Engenharia Química, Universidade Federal Do Ceará, Campus Do Pici, Bloco 709, Fortaleza, CE, CEP 60.455-760, Brazil*
[e] *Instituto de Engenharias e Desenvolvimento Sustentável, Universidade da Integração Internacional da Lusofonia Afro-Brasileira, Campus Das Auroras, Redenção, CE, CEP 62790970, Brazil*
[f] *School of Environment and Science, Griffith University, 170 Kessels Road, Nathan, QLD, 4111, Australia*
[g] *Department of Sanitary Engineering, Faculty of Civil and Environmental Engineering, Gdańsk University of Technology, G. Narutowicza 11/12 Str., 80-233 Gdansk, Poland*
[h] *Advanced Materials Center, Gdansk University of Technology, G. Narutowicza 11/12 Str., 80-233 Gdansk, Poland*

HIGHLIGHTS

- Competitiveness of bismuth-based photocatalysts for hydrogen production.
- Mechanism and thermodynamics of the photocatalytic water splitting.
- Properties of an ideal photocatalyst for water splitting.

ARTICLE INFO

Article history:
Received 10 November 2022
Received in revised form
30 April 2023
Accepted 4 May 2023
Available online xxx

Keywords:
Nanomaterials
Green energy
Z-scheme heterojunction
Nanocomposites

ABSTRACT

The rapidly increase in the world's population has resulted in a corresponding increase in the energy demand. This demand is largely being met by fossil fuels for power generation, industrial fuel and transportation. However, due to the limited availability of fossil fuels and their negative effects on the environment. The use of fossil fuels results in by-products such as carbon, nitrogen and sulfur oxides which have negative impacts on the environment. Therefore. There is an urgent need to develop alternative greener energy sources that are sustainable and have minimal environmental impacts. Hydrogen is one such alternative energy source of attention. Harvesting sunlight through the use of solar panels is already being employed at domestic and commercial levels. Photocatalytic water splitting, which aims to produce hydrogen by utilizing unlimited sources including water and sunlight, is another potential process for alternative energy production. The conversion of water into hydrogen and oxygen through sunlight is an innovative process that directly converts sunlight into chemical energy in the form of hydrogen and oxygen via

* *Corresponding author.*
** Corresponding author.
E-mail addresses: imran.hons@pu.edu.pk (M. Imran), grzegorz.boczkaj@pg.edu.pl (G. Boczkaj).
https://doi.org/10.1016/j.ijhydene.2023.05.047

Please cite this article as: Saddique Z et al., Bismuth-based nanomaterials-assisted photocatalytic water splitting for sustainable hydrogen production, International Journal of Hydrogen Energy, https://doi.org/10.1016/j.ijhydene.2023.05.047

Hydrogen fuel
Sustainable energy

photocatalytic water splitting. Numerous photocatalytic materials are available for photocatalytic hydrogen production, but bismuth-based materials are the most suitable as they are non-toxic, economical, opto-electronically active, have suitable band positions for photocatalysis, and exhibit excellent photo-stability.

To provide summary of latest research in the field of photocatalytic water splitting, a comprehensive review is favorable to suggest future research directions aimed at discovering solutions to current challenges. This review emphasizes the need for alternative energy sources and the competitiveness of photocatalytic water splitting for hydrogen production. The mechanism and thermodynamics of the photocatalytic water splitting have been discussed, along with the properties of an ideal photocatalyst for photocatalytic hydrogen production with a special focus on the bismuth-based photocatalysts. The optimization of synthetic and photocatalytic processes is crucial for commercial use with much improved hydrogen production in terms of cost and quantity without harming environment at any stage. Furthermore, current challenges and future perspectives have been presented for upcoming research in this domain.

Introduction

The conversion of solar energy into hydrogen through photocatalysis is a promising method for obtaining renewable and eco-friendly energy to meet future energy demands. Hydrogen is an exceptional energy carrier due to high energy density (141.8×10^6 J/kg) [1,2], ease of storage and transportation and renewable nature. Additionally, when burned with oxygen, hydrogen only produces water rather than harmful by-products, thus, has potential for use in vehicles, jet propulsions, and power generation [3–7]. The global energy crisis and environmental pollution are two critical issues that hinder social development and threaten our civilization. Since the industrial era, coal and petroleum have been the primarily sources of energy worldwide, but these resources are finite and depleting. To achieve sustainable development, it is necessary to urgently address these problems by transitioning to cleaner and renewable resources, such as green hydrogen production via solar-powered water splitting. The widespread distribution and abundance of solar energy make the solar-powered water splitting a promising green source of energy with minimal environmental impact. It has been reported that the sun emits solar energy equivalent to that produced by 130–500 MW power plants at any given moment [8].

Water is an abundant source of hydrogen, but due to the large distribution of solar energy, it is challenging to split water into stoichiometric hydrogen and oxygen on a commercial scale. However, photocatalysis can be effectively harness solar energy to break down water into its individual elements.

This promising approach is cost effective and non-toxic [9]. Fundamental steps involved in photocatalytic water splitting are: (1) absorption of solar energy by the photocatalyst for electron-hole generation, (2) transfer of charge to the surface of photocatalyst, and (3) hydrogen evolution on the surface. This reaction is only feasible when the potential difference of the photocatalyst exceeds the standard potential difference of water (1.23 eV) [10,11]. Although the scientific community has made progress in optimizing the first two steps, the third step is still a challenge, as it requires a co-catalyst for proper functioning [12]. The surface of photocatalysts undergoes a side reaction called surface back reaction, which results in the recombination of photogenerated hydrogen and oxygen to form water. This reaction negatively affects hydrogen production. To counter this effect, sacrificial reagents and photoactive sites are used. Reports suggested that sacrificial agents are used to enhance the rate of reaction of photoexcited charge carriers and suppress the negative effects of surface back reaction resulting from photon strike on the photocatalyst surface. The sacrificial agents act as external electron donors and acceptors, reducing the likelihoods of surface back reaction. Methanol and ethanol are commonly used sacrificial agents, and the photocatalytic reaction in which they are used is called as a half reaction for hydrogen production [13]. Other reagents such as lactic acid and triethanolamine have also been used to improve hydrogen production [14,15]. However, using additional reagents to maximize production efficiency increases the cost of production process, making it unsuitable for commercial use. Separation of photoactive sites is another method to prevent the recombination of photogenerated hydrogen and oxygen. This step also assists to separate electron-holes pairs, inhibiting their recombination, which leads to better photocatalytic hydrogen production. The morphology of the photocatalyst plays a vital role in execution of this step [15]. An alternative approach to splitting water via sunlight is through photo electrochemical methods. However, this technique requires an additional source of electricity to produce hydrogen, with semiconductors acting as photoanode and photocathode, and external electricity is provided through these electrodes to electrolyze water before splitting [16–18]. Compared to photo electrochemical water splitting, photocatalytic water splitting is a more promising option in terms of performance, cost and environmental friendliness. The former method involves expensive and toxic chemicals and additional electricity making it the process complex, resulting in unsatisfactory outcomes [19–21].

Photocatalytic water splitting involves in the use of semiconductors as photocatalyst, and numerous semiconductors have been researched and developed for photocatalytic water

Please cite this article as: Saddique Z et al., Bismuth-based nanomaterials-assisted photocatalytic water splitting for sustainable hydrogen production, International Journal of Hydrogen Energy, https://doi.org/10.1016/j.ijhydene.2023.05.047

splitting. These include compounds such as TiO_2 [10], ZnS, $CuInS_2$ [22], g-C_3N_4 [23,24], Ag_3PO_4 [25], $SrNbO_3$ [26], Bi_4TaO_8X (X = Cl, Br) [27] as well as composites: TiO_2/CdS [28], ZnO/CdS [29], $K_4Nb_6O_{17}$/CdS [29], Pd–Pt/CdS [30], MOF(Ti)/BP [31], $BiVO_4$/PCN [32] and nanomaterials: TiO_2 [33] CdS, MoS_2–CdS [34], $SrTiO_3$ [35], Au@MoS_2 [36], BiOX (X = Cl, Br, I) [37–39], C@CBO [40]. Elaborative reviews on these materials can be found in references [3,4,19,21,23,41–46]. However, achieving efficient photocatalytic water splitting requires a highly sophisticated photocatalyst that can overcome challenges in water oxidation process. An ideal photocatalyst must have relatively narrow band gap, a negative bottom of conduction band and a positive top of valence band. A narrow band gap enhances solar energy harvesting with the pertinent position for generating electron-hole pair involved in redox reaction. The negative bottom of conduction band facilitates the rapid release of hydrogen, and to promote photo-oxidation reaction whilst the top of valence band needs to be positive than redox potential of water. The scientific community has worked to produce materials with these properties, and there seems to be an agreement that bismuth-based materials have the desired properties for photocatalytic water splitting [19]. Bismuth nanomaterials and bismuth halide perovskites are two important types of materials used for photocatalytic hydrogen production form water amongst the bismuth-based materials. Metal halide perovskites (MHPs) are composed of a monovalent organic or inorganic cation, a bivalent metal such as lead, bismuth, and tin and a halide ion [47,48]. Due to their exceptional features, such as a wide absorption range and long electron-hole diffusion, MHPs are suitable for optoelectronic applications, including photovoltaics and photocatalysis [49–51]. However, their instability in water and the toxicity of lead, which is a common component of MHPs, limit their use in photocatalytic water splitting [52]. To address these issues, bismuth has been utilized as an replacement for lead in MHPs. Bismuth based halide perovskites can avoid the toxicity problem but still suffer from instability in aqueous medium. For instance, the inorganic MHP $Cs_3Bi_2I_9$ has been synthesized and used for photocatalytic hydrogen production, demonstrating the highest hydrogen evolution of 2157.8 $\mu mol h^{-1} g^{-1}$. However, due to the instability of the MHP, this hydrogen evolution reaction had to be performed in ethanol [52]. The instability of bismuth based halide perovskites in water make them unsuitable for photocatalytic hydrogen production form water. For further information, refer to the excellent reviews referenced here [53–56]. In contrast, bismuth based nanomaterials exhibit excellent stability in aqueous media and possess distinctive electronic structures with a relatively narrow band gap and high photo-oxidation intensity. These properties offer a rich source of electrons and photons that can be highly advantageous for the process of hydrogen production via water splitting (as illustrated in Fig. 1) [20,57,58].

This review aims to examine the potential of bismuth-based materials for producing hydrogen through photocatalytic water splitting, as a sustainable, renewable and solar-driven energy source. The review further aims to provide readers with a comprehensive understanding of the synthetic and mechanistic aspects of bismuth-based photocatalysts for this process. It includes recent literature on the topic, highlights current challenges that hinder the upscaling of this technology, and suggests future research directions for further exploration.

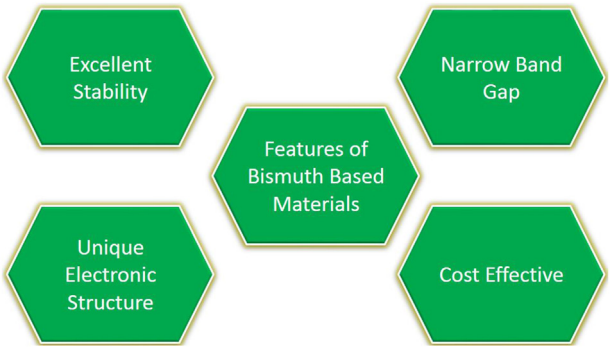

Fig. 1 – Prominent features of bismuth based materials that play significant role in photocatalytic water splitting for hydrogen production.

Water splitting: mechanism and thermodynamic approach

The process of water splitting is involves a dissociation of water into its elemental components; hydrogen and oxygen with the aid of an energy [59]. Several techniques have been utilized to achieve split water for hydrogen production, such as photocatalytic [60], photo electrochemical [4], thermal decomposition [61], radiolysis [62], and photo biological [63] techniques. Photocatalytic water splitting is a process in which water is transformed into stoichiometric hydrogen and oxygen through the conversion of light energy into chemical energy in the presence of a photocatalyst. On the other hand, photochemical/photo electrochemical water splitting requires the use of both photocatalyst and external redox electron source to separate water into oxygen, making them complicated and expensive [4]. Thermal decomposition requires high temperatures (above 2000K) for water splitting, in addition to the fast recombination of hydrogen and oxygen, low yield, and high temperatures are significant drawbacks [61]. Radiolytic water splitting involves irradiating water molecules in the presence of supra-molecular compounds. This process produces not only hydrogen and oxygen but nuclear waste. The use of supra-molecules and production of nuclear waste make this process unattractive [62]. Some photoautotrophic microalgae and cyanobacteria can also produce hydrogen through photobiological water splitting by absorbing sunlight [63]. Amongst the techniques mentioned, photocatalytic water splitting is simplest, most cost-effective, cleanest and efficient technique for hydrogen production using sunlight. Its primary advantage is that there is no possibility of byproduct formation, making it an attractive process for hydrogen generation [64]. Dincer et al., conducted a comparison of various hydrogen production techniques and concluded that photocatalytic water splitting is the most cost-effective and environmentally friendly method. However, despite its advantages, the efficiency of photocatalytic water splitting for hydrogen generation is still sub-optimal levels. To improve the efficiency, materials tailored specifically for photocatalytic

Please cite this article as: Saddique Z et al., Bismuth-based nanomaterials-assisted photocatalytic water splitting for sustainable hydrogen production, International Journal of Hydrogen Energy, https://doi.org/10.1016/j.ijhydene.2023.05.047

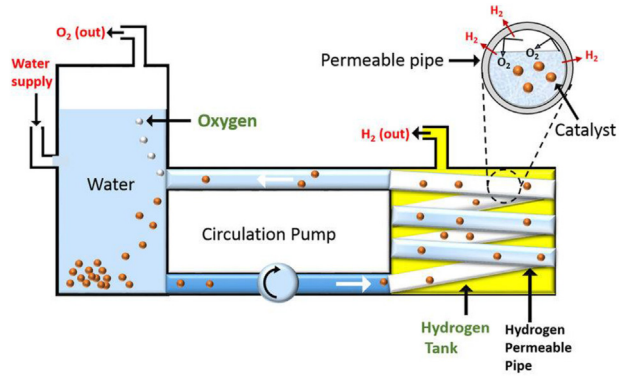

Fig. 2 – Schematic illustration of photocatalytic water splitting for hydrogen production. Reprinted from Ref. [17] with permission from Materials Research Society. Copyright © 2011, Materials Research Society.

water splitting are required, as the efficiency of the process is dependent on the characteristics of the photocatalyst material used [64]. A schematic illustration of semiconductor based photocatalytic water splitting for hydrogen production is presented in Fig. 2.

Photocatalytic water splitting involves the acceleration of oxidation and reduction processes at separate sites, resulting in two distinct stoichiometric products. This process directly converts solar energy into hydrogen energy by utilizing a semi-conductor photocatalyst [65]. The photocatalyst possess a valence band and a conduction band separated by a band gap energy, which determines the photocatalytic properties of the material [66]. Based on the number of steps involved, photocatalytic water splitting is categorized into two mechanisms: one-step photo-excitation mechanism and two-step photo-excitation. The one-step photo-excitation mechanism is a single step process in which a photocatalyst with enough potential to split water into hydrogen and oxygen when the catalysis is exposed to visible light to convert solar energy into chemical energy. Favorable conditions for the one-step mechanism include a narrow band gap of photocatalysis to generate photons, operational environmental and thermodynamic stabilities [67]. Fig. 3 illustrates one-step photo-excitation mechanism of photocatalytic water splitting.

Lee et al., and Maeda et al., highlighted the challenges in achieving the desired properties in materials for a one-step photo-excitation mechanism, leading to limitations in its application [69,70]. However, the two-step photo-excitation mechanism, also known as the Z-scheme mechanism, has addressed the issues related to the one step photo-excitation mechanism. This mechanism resembles natural photosynthesis and facilitates hydrogen and oxygen production through two distinct steps. In the first step, water is oxidized to produce oxygen, while in the second step, hydrogen cations are reduced to form hydrogen molecules. Metal complexes with flexible oxidation states serve as intermediaries to connect these two steps. Compared to the one-step mechanism, the two-step Z-scheme mechanism is much more practical, since it can utilize a wider range of visible light and has a higher likelihood of achieving stoichiometric hydrogen and oxygen [71,72].

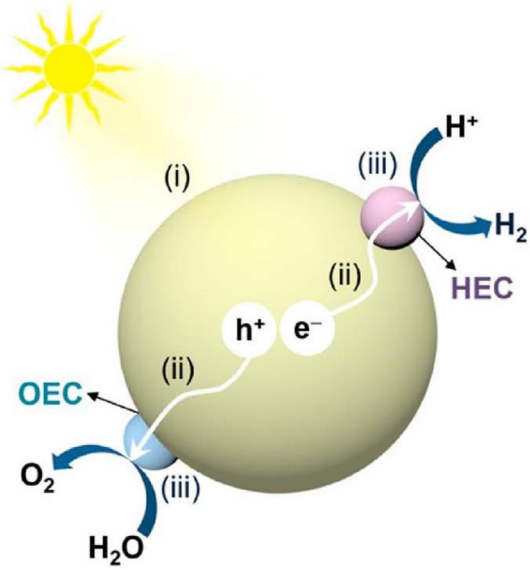

Fig. 3 – General illustration of one step photo-excitation mechanism for photocatalytic water splitting (i) Solar light absorption, (ii) charge separation and charge transfer, (iii) oxidation-reduction reaction. OEC: O_2 evolving catalyst; HEC: H_2 evolving catalyst. Reprinted from Ref. [68] with permission from American Chemical Society. Copyright © 2019, American Chemical Society.

The process of the two-step photo-excitation mechanism for photocatalytic water splitting is illustrated in Fig. 4. In the first step, when photons from the sun interact with the photocatalyst at an energy level equal to or greater than the photocatalyst's band gap, charge carriers including electron/hole (e^--h^+) pairs are produced. The second step involves the separation of these photo-excited charge carriers, which is crucial to avoid recombination of the electron-hole pairs leading to energy dissipation in the form of heat in nanoseconds. These separated photo-excited electron-hole pairs are then transported to the photocatalyst surface to react with water, resulting in the dissociation of water into stoichiometric hydrogen and oxygen. The surface electrons of the photocatalyst are responsible for reducing water to produce hydrogen, whilst the surface holes oxidize water to produce oxygen [74,75]. Eq. (1) and Eq. (2) represent the photo oxidation and reduction reactions occurring during the photocatalytic water splitting process, respectively.

$$\text{Photo} - \text{oxidation} : 2H_2O + h\upsilon \rightarrow O_2 + 4\,H^+ + 4e^- \quad (1)$$

$$\text{Photo} - \text{reduction} : 2H_2O + 2e^- + h\upsilon \rightarrow H_2 + 2OH^- \quad (2)$$

Photocatalysis is determined by various factors from a mechanistic perspective. These include the density of light absorption, the generation of electron-hole pair, the rate of recombination of charge carriers, and the efficient transportation of electron-hole pairs for water oxidation and reduction. The more light absorbed, the greater the production of electron-hole pairs and the faster the photocatalysis process [76].

Please cite this article as: Saddique Z et al., Bismuth-based nanomaterials-assisted photocatalytic water splitting for sustainable hydrogen production, International Journal of Hydrogen Energy, https://doi.org/10.1016/j.ijhydene.2023.05.047

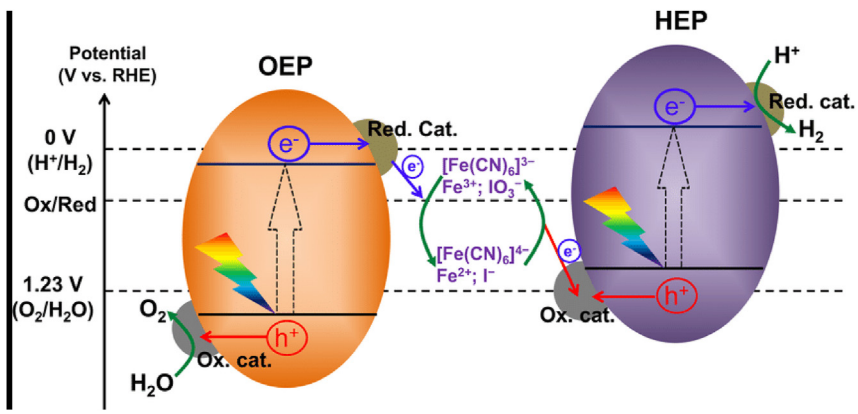

Fig. 4 – Schematic illustration of two step photo-excitation mechanism for photocatalytic water splitting. Reprinted from Ref. [73]. Red. Cat.: reduction co-catalyst; Ox. Cat.: oxidation co-catalyst; RHE: reversible hydrogen electrode; OEP: O_2-evolving photocatalyst HEP; H_2-evolving photocatalyst. This article is licensed under a Creative Commons Attribution 4.0 International License (http://creativecommons.org/licenses/by/4.0/).

Understanding thermodynamics of photocatalytic water splitting is also essential. Li et al., expressed the reaction as an 'uphill' reaction thermodynamically since it requires amount of energy equivalent to the standard Gibbs free energy change ($\Delta G^{\circ} = 237$ kJ/mol) to initial water splitting into stoichiometric hydrogen and oxygen.

$$H_2O \rightarrow H_2 + \frac{1}{2}O \Delta G^{\circ} = +237 \text{ KJ mol}^{-1}; \quad E^{\circ} = 1.23 \text{ eV} \tag{3}$$

$$2H^+ + 2e^- \rightarrow H_2 \quad E^{\circ} = 0 \text{ eV reduction} \tag{4}$$

$$2H_2O \rightarrow 4H^+ + 4e^- + O_2 \quad E^{\circ} = 1.23 \text{ eV oxidation} \tag{5}$$

$$E_{CB} = E^{\circ}_{CB}\,(pH = 0) - 0.059\,pH \tag{6}$$

Eq. (3) describes the complete redox process of water splitting, in which a Gibbs free energy of 237 kJ/mol is required to initiate the reaction by overcoming the energy barrier of 1.23 eV. Eq. (4) indicates that no Gibbs free energy is required for the reduction process, whilst Eq. (5) reveals that overcoming the energy barrier of 1.23eV is necessary for the oxidation process, which is the actual energy barrier for the entire water splitting reaction [77]. Eq. (6) provides the relationship between the band edges of semi-conductor photocatalyst and the pH. In conclusion, a thermodynamically non-spontaneous photocatalytic water splitting can be achieved by adding extra photons to the photocatalyst, providing enough energy to overcome the energy barrier of 1.23 eV, and convert water into hydrogen and oxygen. An ideal photocatalyst should have a band gap greater than 1.23 eV to initiate water splitting. Additionally, to achieve this level of energy, wavelength of the light must be between 400 and 1000 nm otherwise less energy will be generated. These are the prerequisites for generating electron-hole pairs followed by their separation, while for the third step of photocatalytic water splitting (photo-oxidation and photo-reduction), the redox potential of water and band position of photocatalyst should matched. Fig. 5 illustrates the thermodynamics involved in photocatalytic water splitting. To drive the reduction process, the photocatalyst's conduction should be

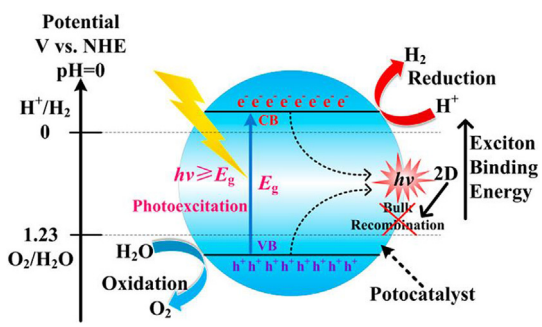

Fig. 5 – Schematic illustration of thermodynamic principles of photocatalytic water splitting. CB; Condcution band, VB; Valence band, E_g; Band gap. Reprinted from Ref. [80] with permission from American Chemical Society. Copyright © 2018, American Chemical Society.

negative relative to the H^+/H_2 (0 eV) redox potential versus the normal hydrogen electrode (NHE) at pH = 0. In the case of oxidation, the photocatalyst's valence band should be more positive than the O_2/H_2O (1.23 eV) oxidation potential relative to NHE at pH = 0. Both the band edges of the photocatalyst and the redox potential of water are pH dependent, with a slope of 0.059 V/pH as shown in Equation (6), Consequently, the overpotential of photo-excited charge carriers has no effect on the redox potential of water at different pH values [75,77–79].

Features of photocatalyst for photocatalytic water splitting

The efficiency of photocatalytic hydrogen production from water is greatly influenced by the electrical and structural properties of photocatalyst. The generation and migration of electron-hole pair in photocatalyst rely on these charged carrier, and the optimization of the electrical and structural characteristics of photocatalyst can impact the efficiency of the process. The introduction of defects and co-catalyst can

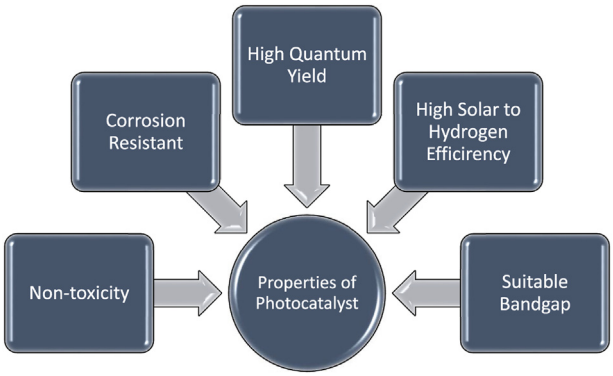

Fig. 6 – Desirable properties of an ideal photocatalyst for hydrogen production form water.

influence the photocatalyst's performance. The presence of defects in the crystal structure of the photocatalyst reduces photocatalytic efficiency since these defects act as sites for the recombination of electron-hole pairs, dissipating energy as heat. It is widely known that hydrogen activation requires a large surface area, which is often absent in most photocatalysts. This limitation can be addressed by adding a co-catalyst to the photocatalyst surface with a size smaller than 50 nm, which provides active sites and initiates hydrogen evolution. The other desired properties for efficient photocatalytic water splitting for hydrogen production are summarized in Fig. 6 [81–83].

Bismuth based materials are highly regarded for their potential in photocatalytic water splitting for hydrogen production due to their unique electronic structure, narrow band gap, non-toxic nature, good reusability, cost effectiveness and good quantum yield [84]. Moreover, bismuth based nanomaterial exhibit exceptionally photostability in addition to their stability in water, thereby addressing a technical challenge faced by semiconductor photocatalysts for hydrogen evolution [85]. Traditional photocatalysts tend to degrade under sunlight due to self-oxidation from photogenerated holes. However, in bismuth base materials, particularly halogen oxides, the elevated 2p band of oxygen dominate the valence band of the photocatalyst, ensuring long term photostability and preventing self-oxidation whilst maintaining suitable band levels [86,87]. Bismuth is particularly effective in photocatalytic water splitting due to the presence of a 6s orbital in the valence bands of bismuth-based materials. The well-dispersed 6s orbital allows for efficient electron-hole pair mobility and reduced band gap. As a result, most of the previous reports on bismuth-based materials have a band gap less than 3 eV, enabling efficient energy harvesting for hydrogen production [88,89]. Additionally, the 6s orbital's delocalization provides exceptional stability to bismuth-based photocatalysts. Several studies have demonstrated that bismuth-based photocatalysts do not require surface modification, as they are photostable, and after repeated application cycles, there is no change in their chemical or physical structure or signs of self-decomposition. The extended lifespan of bismuth-based photocatalysts is a distinguishing factor among various semiconductor-based photocatalysts [86,90,91].

Synthesis of bismuth based materials

Various types of bismuth based materials, including nanomaterials [92], composites [93], compounds [46], hybrids [94] and doped materials [74] have been utilized for photocatalytic water splitting for hydrogen generation. The synthesis of bismuth-based materials involves several techniques, such as solvothermal, hydrothermal, sol-gel, solid-state reaction, and sonochemical methods In the solvothermal method, the precursors are dispersed in solvents such as ethylene glycol and glycerol and placed in a mild temperature ranging from 80 to 180 °C for 12–24 h in an autoclave. Pressure is buildup in the autoclave due to the elevated temperature, and the reaction occurs due to the increased pressure [95]. In the hydrothermal method, water is used as the solvent, while the remaining procedure is similar to the solvothermal method [96]. In sol-gel method of semiconductor synthesis, a gel of suitable material is prepared as a precursor, and the precursor is reduced into a semiconductor inside of the gel. This method allows for easy separation of the as-produced material [74]. In the solid-state reaction, the reactants are ground and heated at high temperatures (over 1000 °C). However, the need for such a high temperature makes this method unfavorable and expensive [97]. Among these methods, the hydrothermal method is favorable due to its yield, tunability of morphology and size of the crystalline phase through varying solvents, and cost-effectiveness. However, issues related to by-product formation need to be addressed for practical applications. This section provides an overview of different synthesis methods for various classes of bismuth-based materials.

Bismuth-based nanomaterials

Wang et al. utilized the exceptional photocatalytic properties of bismuth nanoparticles to synthesize Bi_3NbO_7 nanoparticles. They employed a hydrothermal method combined with the assistance of a polymerization complex. To achieve this, niobic acid was dissolved in oxalic acid and bismuth nitrate pentahydrate was added until a white milky suspension formed. The mixture was then heated at 120 °C in an autoclave for 12 h. The resulting product was washed with deionized water and alcohol to remove impurities before being dried. This product was then used as a photocatalyst in photocatalytic water splitting without any further treatment [96]. Another study prepared $BiVO_4$ nanocrystals using a solution combustion technique This involved reacting bismuth nitrate pentahydrate and ammonium vanadate in the presence of nitric acid and maleic acid, followed by heating up to 500 °C [98]. To synthesize quantum $BiVO_4$ a hydrothermal method was adopted. The reactants were dispersed in deionized water and heated at 100 °C for 12 h, resulting in a tube-like morphology with an estimated diameter of 5 nm, as shown in Fig. 7 [99].

Bismuth nanomaterials containing tungsten oxide have been identified as promising photocatalysts for the process of water splitting. Various morphologies of Bi_2WO_6 have been successfully synthesized through hydrothermal methods, including monolayer Bi_2WO_6 [100] and flower like Bi_2WO_6

Please cite this article as: Saddique Z et al., Bismuth-based nanomaterials-assisted photocatalytic water splitting for sustainable hydrogen production, International Journal of Hydrogen Energy, https://doi.org/10.1016/j.ijhydene.2023.05.047

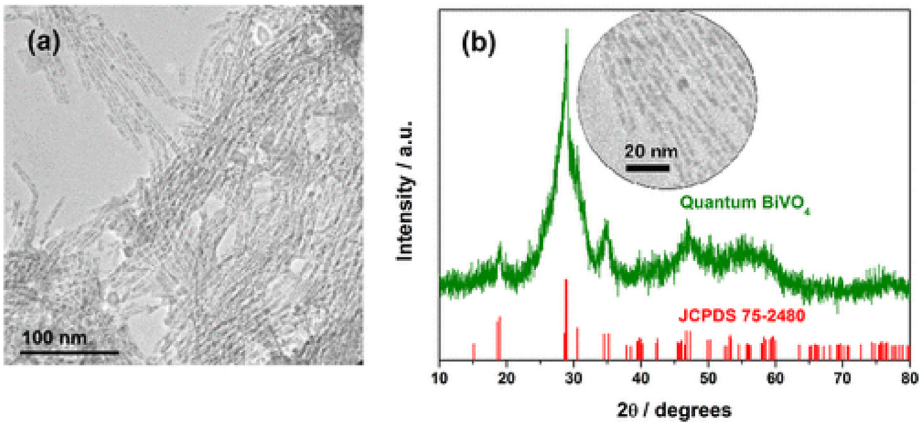

Fig. 7 – (a) TEM images and (b) XRD pattern of $BiVO_4$. Reprinted from Ref. [99] with permission from American Chemical Society. Copyright © 2014, American Chemical Society.

[101], for use in photocatalytic water splitting. Li et al. have reported the successful synthesis of bismuth oxychloride nanosheets through sonication-assisted hydrothermal methods, using bismuth nitrate and potassium chloride as the main precursors. Hydrothermally synthesized NiO_X using nickel nitrate as a precursor was used as a co-catalyst for hydrogen production [102]. Using a solvothermal method, Ye et al. synthesized ultrathin nanosheets of bismuth oxy chloride nanosheets with increased spacing. They dissolved bismuth and chloride precursors separately in glycerol, and added a KCl solution to the bismuth nitrate solution. After transferring the suspension to an autoclave and maintaining it at 160 °C for 16 h, they obtained a black bismuth oxy chloride product which was then purified through centrifugation and washing with ethanol to remove impurities [95]. Similarly, Zhang et al. prepared BiOCl ultrathin nanosheets measuring 3.6 nm in size, and doped them with NiO_X to produce hydrogen through water splitting. The hydrogen evolution rates of both doped and undoped photocatalysts were compared, and it was observed that the simple BiOCl ultrathin nanosheets demonstrated improved performance [103]. One study utilized a reverse micelle-based method without a template to synthesize $Bi_2Ti_2O_7$ nanorods with a diameter of 40–50 nm for photocatalytic water splitting. Bismuth hydroxide and titanium hydroxide were prepared by reverse micelle method, and the resulting product was calcined at 500 °C to produce 20 nm spherical nanoparticles. Further calcination at temperature of 650C caused the nanoparticles to rearrange into nanorods of $Bi_2Ti_2O_7$ [104]. In another study, $BiOIO_3$ nanoplates with a diameter of 25 nm were synthesized using a hydrothermal method. Bi $(NO_3)_3 \cdot 5H_2O$ was dissolved in deionized water, and $NaIO_3$ was added to the solution. The reaction mixture was then heated in a stainless steel autoclave lined with Teflon at 160 °C for 5 h [105]. Yang et al. synthesized $BiFeO_3$ through a sol-gel process and doped with Gd. Bismuth nitrate and ferric nitrate were used as precursors for synthesis of $BiFeO_3$ whilst gadolinium nitrate was used as a doping agent. The doped bismuth ferrite exhibited better stability and performance than the simple bismuth ferrite, as the doped product yielded three times the rate of hydrogen production [74]. Bismuth-based photocatalysts for water splitting have been synthesized using combustion, sol-gel, solvothermal, and hydrothermal methods. The hydrothermal approach reportedly provided higher conversion efficiency, was less time-consuming, and did not require additional reagents.

Bismuth-based composites

Bismuth-based composite materials prepared with other materials such as metals, metal oxides, carbon quantum dots, graphitic carbon nitrides, have demonstrated further enhanced efficiency in photocatalytic hydrogen production. The BiOCl/CuPc composite, for example, was synthesized using a solvothermal method that involved dissolving bismuth nitrate in ethylene glycol and preparing a CuPc solution using methoxyethanol. The two solutions were then mixed and heated at 120 °C for an hour to produce the blue-colored BiOCl/CuPc composite, which was used for hydrogen production [106]. Another example of a composite material for photocatalytic water splitting is the BiOCl/Au/MnOx composite, which was synthesized by photo-depositing gold and manganese oxide onto hydrothermally synthesized BiOCl nanosheets. This composite material was also used for hydrogen production, as reported by Zhang et al. [107]. Nd/Bi_2O_3 composite photocatalysis was synthesized by Al. Namasha et al. for hydrogen production. They added Bi_2O_3 nanosheets to neodymium nitrate solution and exposed the mixture to visible light for 24 h. Excess ethanol was then removed by vacuum heating at 333K for 10 h [108]. Li et al. developed MoS_2/$Bi_{12}O_{17}C_{l2}$ bi-layer nanocomposite for photocatalytic hydrogen evolution. Firstly, $Bi_{12}O_{17}C_{l2}$ was synthesized by mixing and stirring of bismuth trichloride with ethanol to form yellow precipitates, followed by adding a few drops of sodium hydroxide. Yellow crystals were calcined at 450 °C to obtain $Bi_{12}O_{17}C_{l2}$ nanosheets. Secondly, MoS_2 nanosheets were prepared by mixing $(NH_4)_6Mo_7O_{24} \cdot 4H_2O$ and thiourea, followed by autoclaving at 200 °C for 24 h under autogenous pressure. The resulting MoS_2 nanosheets were washed with ethanol/deionized water. After preparing monolayers of MoS_2 and $Bi_{12}O_{17}C_{l2}$, the layers were assembled into a bi-layer nanocomposite using a sonicator under argon gas for deoxygenation. The mixture

Please cite this article as: Saddique Z et al., Bismuth-based nanomaterials-assisted photocatalytic water splitting for sustainable hydrogen production, International Journal of Hydrogen Energy, https://doi.org/10.1016/j.ijhydene.2023.05.047

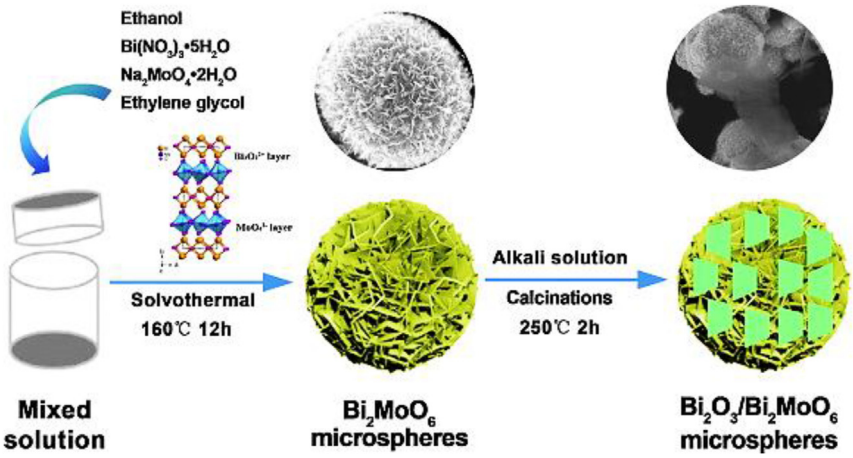

Fig. 8 – Synthetic mechanims of Bi_2O_3/Bi_2MoO_6 composites for photocatalytic hydrogen production. Reprinted from Ref. [128] with permission from Elsevier. License Number: 5424260484398.

was then refluxed at 80 °C and washed with a water-ethanol solution to obtain the final product [109]. Reduced graphene oxide, also known as monolayer graphite, is attracting significant attention for its unique electronic properties, 2D structure, increased surface area, and excellent electron transport capabilities [110]. These properties make graphene oxide an attractive material for the creation of bismuth composites used in photocatalytic water splitting. One such example is the hydrothermal synthesis of a $BiPO_4$/rGO, in which graphite oxide and bismuth phosphate were dispersed in water and heated to 60 °C [111]. Another composite Another composite was synthesized through an electrospinning method, in which bismuth molybdate was combined with graphene oxide [112]. Sun et al., developed nanocomposites of Bi_2WO_6 on graphene oxide for photocatalytic hydrogen production. To produce these nanoparticles, $Bi(NO_3)_3 \cdot 5H_2O$ was dissolved in water and treated with HNO_3, followed by the addition of graphene oxide. The resulting mixture was heated at 450 °C for 3 h to form black crystalline Bi_2WO_6/GO [113]. Various composites based on Bi_2WO_6 have been synthesized through hydrothermal and electrospinning calcination methods, including BP/Bi_2WO_6 [114], TiO_2/Bi_2WO_6 [115], $Bi_2O_2CO_3/Bi_2WO_6$ [116] and CdS/Bi_2WO_6 [117]. Other materials used for photocatalytic water splitting, such as Bi_2WO_6/GO [118] and Bi_2WO_6/BiO [119], have been synthesized using solvothermal and hydrothermal methods in which the precursor materials are dissolved in a suitable solvent and heated at an appropriate temperature for a specific duration. $BiVO_4$ based composites have also been reported as photocatalyst for water splitting, including $ZnIn_2S_4/BiVO_4$ [120], NiO/CDs/$BiVO_4$ [121], $SrTiO_3$:La,Rh/Au/$BiVO_4$:Mo [122], $Cd_{0.5}Zn_{0.5}S/BiVO_4$ [123] and BP/$BiVO_4$ [124], all synthesized using a facile hydrothermal method. Due to its narrow band gap (2.7 eV) and structural stability, graphitic carbon nitride has been utilized for photocatalytic hydrogen production through its composite formation with metal oxides [125]. For example, Bi_2MoO_6/g-C_3N_4 was synthesized via a solvothermal process in which the precursors were dissolved in ethanol and heated in an autoclave at 160 °C for 5 h [126]. Zhang et al., reported a one-step hydrothermal method for synthesizing CQDs/Bi_2MoO_6, in which metal precursors were dissolved in deionized water and heated at 160 °C for 24 h. The resulting composites were used in photocatalytic hydrogen production [127]. Recently, solvothermally synthesized $BiMoO_4$ was utilized to produce Bi_2O_3/Bi_2MoO_6 through an alkali treatment method followed by air calcination for the photocatalytic hydrogen production [128]. However, the methods reported in the literature for synthesizing bismuth-based photocatalysts have limitations in terms of uncontrollable morphology and structure. These methods require harsh conditions and technicalities that limit the tunability of process parameters. There is a need to develop a method for tailoring desirable deatures for hydrogen production at an industrial scale. Fig. 8 illustrates the two steps involved in the synthesis of Bi_2O_3/Bi_2MoO_6.

Bismuth-based compounds

Various techniques have been utilized to synthesize bismuth compounds that have been reported as photocatalysts for water splitting. Lee et al. recently reported the synthesis of bismuth oxyhalides BiOX (X = Cl, Br, I) via a microwave assisted solvothermal method to produce a hierarchical microsphere product with a flower-like morphology. The synthesized bismuth composites were employed for water splitting to produce hydrogen. It was discoverd that BiOI displayed the highest photocatalytic activity among all BiOX, owing to its low bandgap of 2.04 eV [38]. Shang et al. utilized a chemical precipitation method to synthesize $Bi_{24}O_{31}Br_{10}$ powders using two solutions, one acidic and the other alkaline. The acidic solution was prepared by dissolving Bi $(NO_3)_3 \cdot 5H_2O$ in dilute HNO_3, while the alkaline solution was prepared by dissolving hexadecyl trimethyl ammonium bromide (CTAB) in an aqueous NaOH solution. The alkaline solution was added dropwise to the acidic solution while it was being stirred on a magnetic stirrer, resulting in the formation of yellow-green precipitates. The precipitates were filtered, washed, and subjected to heating at different temperatures to obtain the desired powder [129]. Kudo et al. developed eight distinct bismuth-based compounds for photocatalytic water splitting purposes. These photocatalysts, including $Bi_2W_2O_9$, Bi_2WO_6, $Bi_{14}W_2O_{27}$, $Bi_2Ti_2O_7$, Bi_3TiNbO_9, $Bi_4Ti_3O_{12}$, $BiMoO_6$ and $BaBi_4Ti_4O_{15}$, were synthesized via solid-state reactions

Please cite this article as: Saddique Z et al., Bismuth-based nanomaterials-assisted photocatalytic water splitting for sustainable hydrogen production, International Journal of Hydrogen Energy, https://doi.org/10.1016/j.ijhydene.2023.05.047

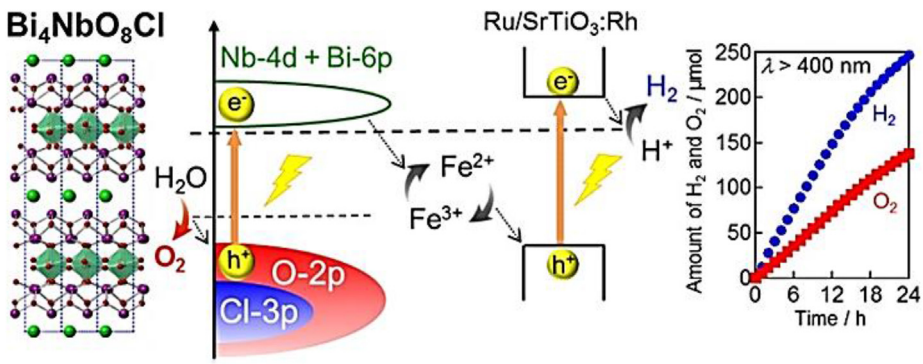

Fig. 9 – Visible light active layered perovskite Bi_4NbO_8Cl synthesized through solid state reaction for the photocatalytic hydrogen production. Reprinted from Ref. [86] with permission from American Chemical Society. Copyright © 2016 American Chemical Society.

utilizing Bi_2O_3, TiO_2, Nb_2O_5 WO_3 and $BaCO_3$ as starting materials at different calcination temperatures [130]. Of these compounds, only two were capable of splitting water but could solely generate stoichiometric oxygen rather than hydrogen. Consequently, these compounds were not suitable for hydrogen production. Bismuth compounds combined with other metal oxides have also been created for photocatalytic water splitting. Among the compounds, $PbBi_2Nb_2O_9$ is a reported compound that was synthesized via solid-state reaction using PbO, Bi_2O_3 and Nb_2O_5 as starting materials. The resulting powder was then calcined at temperatures ranging from 1273 to 1473 K for 48 h [131,132]. Liu et al., synthesized $BiYWO_6$ via a solid state reaction, using WO_3, Y_2O_3, and Bi_2O_3. The reaction mixture was then calcined at 1323–1373 K for 24 h. The resulting product was used in water splitting for hydrogen production [97]. It has been discovered that the presence of the 2p orbital of oxygen in photocatalysts, such as Bi_4NbO_8Cl, lead to high dispersion, narrow band gap, and relatively higher stability, which are two of the most advantageous qualities in an ideal photocatalyst. Bi_4NbO_8Cl was synthesized through a solid-state reaction between Bi_2O_3, BiOCl and Nb_2O_5, by heating reactants at 1173K for 20 h (as illustrated in Fig. 9) [86]. An alternative synthesis method is the citrate polymeric approach, which utilizes citric acid as a chelating agent and ethylene glycol as the reaction solvent. $BiNb(Ta)O_4$ is an example of such a photocatalyst synthesized using citric acid [133]. However, the production of bismuth-based bulk compounds through these methods can require expensive reagents and harsh conditions, resulting in cost ineffective photocatalysts that may not be suitable for large-scale industrial applications. Additionally, unknown byproducts may compromise the purity of the photocatalyst.

Non-stoichiometric compounds of bismuth

A scheelite type compound that contains non-stoichiometric bismuth has been synthesized for hydrogen production from water splitting. The synthesis was achieved through solid-state methods using oxide and carbonate starting materials at various calcination temperatures. The products consist of

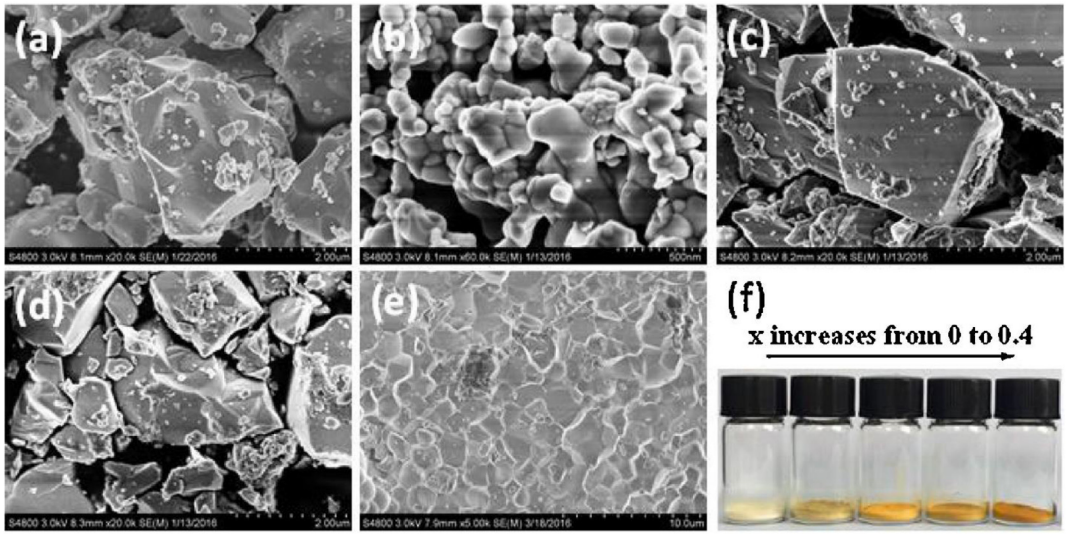

Fig. 10 – FESEM images of $Sr_{1-x}Bi_xTi_{1-x}Fe_xO_3$ having different morphology with varying value of x (a) x = 0, (b) x = 0.1, (c) x = 0.2, (d) x = 0.3, (e) x = 0.4 and (f) images of product in powder form. Reprinted from Ref. [135] with permission from Elsevier. License Number: 5453600639286.

Please cite this article as: Saddique Z et al., Bismuth-based nanomaterials-assisted photocatalytic water splitting for sustainable hydrogen production, International Journal of Hydrogen Energy, https://doi.org/10.1016/j.ijhydene.2023.05.047

bismuth in non-stoichiometric form [134]. Similarly, Lu et al. utilized the conventional technique of solid state reaction to synthesize $Sr_{0.9}Bi_{0.1}Ti_{0.9}Fe_{0.1}O_3$ and $Sr_{0.6}Bi_{0.4}Ti_{0.6}Fe_{0.4}O_3$ as photocatalyst in water splitting for hydrogen production [135,136]. Fig. 10 displays the morphological characteristics of various compositions of $Sr_{1-x}Bi_xTi_{1-x}Fe_xO_3$.

A sol-gel synthetic technique was used to prepare non-stoichiometric nano-crystallites of $Bi_2Ga_{3.6}Fe_{0.4}O_9$, whereby $Fe(NO_3)_3 \cdot 6H_2O$, Bi_2O_3 and Ga_2O_3 were dissolved in a mixture of nitric and citric acid. The reaction mixture was then heated at 670 °C to obtain a pure product [93]. Wang et al. synthesized the non-stoichiometric compound $Bi_{0.5}Na_{0.5}TiO_3$ to enhance photocatalytic hydrogen production from water splitting by harnessing the band gap narrowing effect of Bi^{3+} in the formation of metal oxides containing bismuth. To synthesize the photocatalyst, Bi $(NO_3)_3 \cdot 5H_2O$, Ti $(OC_4H_9)_4$ and NaOH as precursors through a hydrothermal method [137]. Kanhare et al. also sued solid-state reaction method to dope $NaTaO_3$ with bismuth (Bi^{3+}) for developing a photocatalyst for hydrogen production [138]. The presence of non-stoichiometric bismuth in photocatalytic materials can enhance their photocatalytic activity. As such, a study was conducted on $Na(Bi_{0.08}Ta_{0.92})O_3$, to explore this feature in which bismuth was used to enhance photocatalytic activity of the material. The photocatalyst was synthesized hydrothermally using Ta_2O_5, NaOH and $NaBiO_3$ via a typical procedure and heated at 240 °C for 24 h [139]. Transition metals possess the ability to exhibit multiple oxidation states. Additionally, their non-stoichiometric presence in a photocatalyst can enhance its photocatalytic activity. For example, $Bi_4Ti_{2.6}Cr_{0.4}O_{12}$ nanosheets were synthesized by using typical hydrothermal and sol-gel methods [140,141]. A solid solution of $Bi_{0.5}Dy_{0.5}VO_4$ was also prepared using a solid state reaction with Bi_2O_3, Dy_2O_3 and NH_4VO_3 as starting materials, calcined at 1073–1123 K for 24 h [142,143]. Liu et al. synthesized a series of solid solutions having non-stoichiometric photocatalyst $Bi_xY_{1-x}VO_4$ through hydrothermal and solid state reactions for photocatalytic water splitting [144–148]. Wang et al. prepared a bismuth based multi-metal oxide solid solution with a similar non-stoichiometric composition of $Bi_{0.5}Sm_{0.5}VO_4$ through solid state reactions. They replaced yttrium with samarium to produce a photocatalyst for water splitting [149]. Solid state reactions require extremely high temperature to convert reactants into the final product. However, controlling the non-stoichiometric components of the photocatalyst is a challenging task, which is currently one of the most significant issues.

Band gap engineering of bismuth-based materials

Various techniques for engineering the band gap of bismuth-based photocatalytic materials have been described in the literature, including photosensitization, elemental doping, the bismuth-rich approach, and heterojunction formation. Photosensitization involves using light-sensitive materials such as carbon dots, porphyrins, and phthalocyanine to improve sunlight absorption, especially in the visible range. This results in more hydrogen generation and acts as an additional energy source for the photocatalyst [150,151]. Carbon dots, for example, were employed to sensitize bismuth vanadate, which led to increased water splitting and hydrogen production. This technique was shown to be highly effective in enhancing hydrogen production [152]. Doping refers to the introduction of elements into a photocatalyst to enhance its performance, with transition metals being the most commonly used dopants. For instance, tungsten doping in $BiVO_4$ narrows the band gap of photocatalyst by elevating its Fermi level, resulting in enhanced production of hydrogen. In addition, dopant materials increase the redox potential of charge carriers by promoting their separation and reducing recombination [153]. Copper was also used as a dopant in a similar example, with only 20% of Cu doped into MoS_2/Bi_2S_3 leading to improved photocatalytic performance and increased hydrogen production compared to the pristine photocatalyst [154]. The level of conduction band and band gap in a photocatalyst material depends on the amount of bismuth present. Bismuth-rich strategies are used to "tune" the band gap of the photocatalyst, thereby increasing hydrogen production. Multiple studies have shown that the bismuth-rich approach is a promising method for modulating the band gap for photocatalytic water splitting [19,155,156]. To further enhance the photocatalytic activity of semiconductor materials, they are often coupled with other semiconductors with narrower band gaps, resulting in the formation of a heterojunction with a modulated band gap. For instance, $ZnRh_2O_4/Ag/p\text{-}Bi_4V_2O_{11}$ heterojunction was synthesized to increase photocatalytic water splitting for hydrogen production and the results indicated that the resulting catalyst has potential for practical applications. In addition to modulating the band gap, heterojunction composites can also reduce recombination by introducing charge trapping sites and increasing the surface area for sunlight absorption [157]. The average lifetime of a photogenerated electron-hole pair is typically only a few hundred picoseconds [158,159]. However, trap sites in the photocatalyst can restrict the recombination of charges, prolonging their lifetime for the target reaction of hydrogen production. These trap sites also play a role in controlling the diffusion coefficients of photoexcited charges [160,161]. Photosensitization does not significantly alter the band gap, whereas doping and bismuth-rich strategies merely modulate the band gap. On the other hand, composite formation not only modulates the band gap to a desirable level but also provides the additional benefits of increased surface area and reduced charge recombination. Conclusively, heterojunction formation is a highly effective technique for enhancing photocatalytic water splitting.

Bismuth-based materials for water splitting

A variety of bismuth-based photocatalysts have been synthesized and used for water splitting to produce hydrogen as an alternative fuel. The hydrogen yield depends on two factors: the band gap and band edge position of the photocatalyst. A narrow band gap facilitates maximum sunlight absorption, while a suitable band edge position is necessary to prevent recombination of the electron-hole pair and initiate the water splitting reaction. However, literature surveys have

Please cite this article as: Saddique Z et al., Bismuth-based nanomaterials-assisted photocatalytic water splitting for sustainable hydrogen production, International Journal of Hydrogen Energy, https://doi.org/10.1016/j.ijhydene.2023.05.047

indicated that a single photocatalyst cannot provide the optimal band gap and band position to achieve maximum hydrogen yield. Therefore, multi-metal component systems are ideal for water splitting because they efficiently fulfill the aforementioned conditions for photocatalytic water splitting. There are numerous studies where bismuth compounds have been utilized for this purpose either alone or in combination with different types of materials to obtain the maximum benefits. The following paragraphs discuss the influence of band gap and band position on hydrogen yield in bismuth-based nanomaterials, composites, compounds, and non-stoichiometric compounds. For instance, $BiVO_4$ has a narrow band gap of 2.52 eV and produced the highest hydrogen yield of 195.5 μmol h^{-1} under a xenon lamp. Its band gap indicates strong absorption of the porous nano powder in visible light region [98]. Several studies have explored the impact of band gap and band position on hydrogen yield in bismuth-based photocatalytic materials. For example, coupling bismuth with the higher band gap photocatalyst TiO_2 to modulate its band gap for water splitting resulted in a doubling of hydrogen production compared to pristine TiO_2, highlighting the importance of band gap modulation While the narrow band gap of nanomaterials is a determining factor, the influence of band structure cannot be ignored. The band structure has a significant impact on hydrogen yield, as demonstrated by $BiOIO_3$ [105], which has a slightly lower yield than $BiVO_4$ nanoparticles, despite having a band difference of only 0.68 eV. Although several nanomaterials, such as Bi_3NbO_7 [96], $Bi_2Ti_2O_7$ [104], have a narrow band gap, they have obtained low yield of hydrogen. It can be concluded that while band gap is an important factor in nanomaterials for photocatalytic water splitting, band position also plays a significant role in efficiency. To achieve suitable band structures in bismuth-based materials, composites are synthesized. Composite materials have the unique ability to delay rapid recombination of electrons and holes, enhancing the efficiency of the photocatalytic process. In composites, the influence of band gap is negligible, and band structure becomes the determining factor. For example, in $ZnIn_2S_4/BiVO_4$, reactive sites are precisely regulated for photocatalytic water splitting, resulting in a high yield of 5944 μmol h^{-1} g^{-1} of hydrogen [120]. Hetero-interfaces are utilized in bismuth-based materials to accelerate the separation and migration of charge carriers, which enhances the ability of holes to oxidize and electrons to reduce. These changes in band structure result in better hydrogen production compared to other composites, such as $Bi_2O_2CO_3/Bi_2WO_6$ [116], CdS/Bi_2WO_6 [117] andTiO_2/Bi_2WO_6 [115]. Composites also offer the benefit of surface modification for better performance. Surface modification reduces electron-hole recombination and increases hydrogen production with increased quantum yield. This phenomenon was observed in $SrTiO_3$:La,Rh/Au/$BiVO_4$:Mo, where hydrogen production reached at 4750 μmol g^{-1} h^{-1} with conversion efficiency of 1.1% and quantum yield exceeding 30% [122]. In bulk bismuth-based compounds, the impact of band gap on photocatalytic performance is either negligible or non-existent. Instead, band structure modification has been shown to enhance photo-induced charge generation and migration rates, leading to improved hydrogen production. For example, $Bi_2Y_2NbO_8Cl$ exhibited a maximum yield of hydrogen of 113 μmol h^{-1} due to its modified structure [162]. Another important factor influencing photocatalytic water splitting is the molecular structure of the material. Bi_3TiNbO_9, with its slabs like layered structure, exhibited increased surface area, resulting in higher hydrogen generation of 33 μmol g^{-1} h^{-1} [130]. Narrowing the band gap of a photocatalyst material can be achieved through the production of non-stoichiometric compounds, as shown in Table 1 where almost all bismuth-based compounds have a band gap of less than 3 eV. In non-stoichiometric bismuth based photocatalysts, both band gap and band structure play a significant role in determining photocatalytic efficiency, although the balance tilts slightly towards band structure, which has a greater influence than the band gap. Among the non-stoichiometric photocatalysts, $Bi_{0.5}Y_{0.5}VO_4$ demonstrated the highest photocatalytic performance, producing 402 μmol h^{-1} of hydrogen while having band gap of 3.02 eV [144]. The influence of band structure on the photocatalytic properties of photocatalysts is more significant than band gap, as demonstrated by comparison of $Bi_{0.5}Y_{0.5}VO_4$ [144] and $Bi_{0.5}Na_{0.5}TiO_3$ [137]. Despite having a similar band gap, their band structure is completely different, $Bi_{0.5}Y_{0.5}VO_4$ performs better due to its more suitable band structure. Another example supporting the significance of band structure is the increased hydrogen production by non-stoichiometric compound $Bi_{0.5}Sm_{0.5}VO_4$, which has band gap of more than 3 eV but a more stable band structure, resulting in hydrogen production of 188.25 μmol g^{-1} h^{-1} [149]. Table 1 summarizes recently synthesized bismuth-based photocatalyst material used for photocatalytic water splitting Upon comparing their photocatalytic performance, it becomes clear that bismuth-based composites are superior photocatalysts for hydrogen production through water splitting. Notably, $ZnIn_2S_4/BiVO_4$ has demonstrated the highest yield of 5944 μmol h^{-1} indicating excellent photocatalytic performance [120]. Band structure appears to be more important for photocatalytic water splitting than band gap, as supported by the data presented in Table 1. However, there are several challenges hindering the industrial-scale up-scaling of water splitting, such as low sunlight absorption, poor light-to-chemical energy conversion, low charge separation, and high recombination rates, expensive synthetic methods, and difficulties in manipulating the mechanism for higher hydrogen production. Despite this, composites have shown excellent performance due to their modulated band gap, low charge recombination, and larger interfacial surface area. Addressing the challenges in synthesis methods and focusing on positive manipulation of the water-splitting mechanism can revolutionize the field and enable this process to meet the hydrogen demand at an industrial scale.

Current challenges and future recommendations

Currently, photocatalytic water splitting faces two significant challenges: the synthesis of photocatalysts and the photocatalytic mechanism (as shown in Fig. 11). The synthesis of photocatalysts is often expensive and time consuming requiring high processing temperatures in some cases.

Please cite this article as: Saddique Z et al., Bismuth-based nanomaterials-assisted photocatalytic water splitting for sustainable hydrogen production, International Journal of Hydrogen Energy, https://doi.org/10.1016/j.ijhydene.2023.05.047

Table 1 – Bismuth-based material employed for photocatalytic hydrogen production from water splitting.

Sr. No.	Bismuth-based materials	Band Gap	Hydrogen production	Light source	Ref.
Bismuth-based Nanomaterials as a photocatalyst for hydrogen production					
1	Bi_3NbO_7	2.72 eV	110.7 mmol g^{-1} h^{-1}	Xenon lamp $\lambda \geq 420$ nm	[96]
2	$BiVO_4$	2.52 eV	195.6 μmol h^{-1}	Hg–Xe lamp	[98]
3	Q-$BiVO_4$	2.72 eV	0.2 μmol h^{-1}	Xenon lamp	[99]
4	monolayer Bi_2WO_6	2.7 eV	1.6 μmol h^{-1} g^{-1}	Hg Lamp $\lambda > 420$ nm	[100]
5	Flower Like Bi_2WO_6	2.81 eV	7.40 mmol h^{-1} g^{-1}	Xenon lamp $\lambda > 420$ nm	[101]
6	$Bi_2Ti_2O_7$	2.88 eV	140 ml	UV–vis light	[104]
7	$BiOIO_3$	3.2 eV	133 μmol g^{-1} h^{-1}	Xenon Lamp	[105]
8	$NaTaO_3$:Bi^{3+}	2.64 eV	0.86 μmol g^{-1} h^{-1}	Xenon lamp $\lambda > 390$ nm	[138]
9	$BiFeO_3$	2.28 eV	21.9 μmol cm^{-2} h^{-1}	Sunlight	[74]
10	$BiFeO_3$:Gd^{3+}	2.17 eV	67.6 μmol cm^{-2} h^{-1}	Sunlight	[74]
11	BiOCl	3.20 eV	0.35 μmol h^{-1}	Xenon lamp	[103]
12	NiO_x-BiOCl	–	0.10 μmol h^{-1}	Xenon lamp	[103]
13	BiOCl	–	2.51 μmol h^{-1}	Xenon lamp $\lambda \geq 420$ nm	[95]
14	NiO_x-BiOCl:C	–	0.42 mmol g^{-1} h^{-1}	Xenon Lamp	[102]
Bismuth-based composites as a photocatalyst for hydrogen production					
15	BiOCl/Pt	–	0.18 μmol h^{-1}	Xenon lamp $\lambda \geq 420$ nm	[95]
16	BiOCl/Pt	–	3.96 μmol h^{-1}	Xenon lamp $\lambda \geq 420$ nm	[95]
17	BiOCl/Au/MnO_x	–	1.7×10^{-2} mmol g^{-1} h^{-1}	Xenon lamp	[107]
18	BiOCl/CuPc	–	16 μmol g^{-1} h^{-1}	Xenon Lamp	[106]
19	Nd/Bi_2O_3	1.95 eV	250 μmol g^{-1}	Xenon lamp $\lambda > 420$ nm	[108]
20	MoS_2/$Bi_{12}O_{17}C_{l2}$	–	33 mmol g^{-1} h^{-1}	Xenon lamp $\lambda > 420$ nm	[109]
21	$BiPO_4$/RGO	–	30.8 μmol h^{-1}	Hg–Xe lamp	[111]
222	$BiMoO_4$/RGO	2.61 eV	794.72 μmol h^{-1}	Xenon lamp $\lambda > 420$ nm	[112]
23	Bi_2WO_6/GO	–	159.5 μmol h^{-1}	Xenon lamp $\lambda > 420$ nm	[113]
24	Black Phosphorus/Bi_2WO_6	–	350 μmol h^{-1}	$\lambda > 420$ nm	[114]
25	TiO_2/Bi_2WO_6	2.70 eV	11.58 mmol g^{-1} h^{-1}	Xenon Lamp $\lambda \geq 420$ nm	[115]
26	$Bi_2O_2CO_3$/Bi_2WO_6	–	664.5 μmol g^{-1} h^{-1}	Xenon Lamp $\lambda \geq 420$ nm	[116]
27	CdS/Bi_2WO_6	2.11 eV	1223 μmol $h^{-1}g^{-1}$	Xenon Lamp $\lambda \geq 420$ nm	[117]
28	Bi_2WO_6/GO	2.48 eV	78 μmol h^{-1} g^{-1}	Hg Lamp	[118]
29	Bi_2WO_6/BiO	2.44 eV	73 μmol h^{-1} g^{-1}	Xenon lamp	[119]
30	$ZnIn_2S_4$/$BiVO_4$	–	5944 μmol h^{-1} g^{-1}	Xenon Lamp $\lambda \geq 420$ nm	[120]
31	NiO/CDs/$BiVO_4$	2.76 eV	1.21 μmol h^{-1}	Xenon Lamp $\lambda \geq 420$ nm	[121]
32	$SrTiO_3$:La,Rh/Au/$BiVO_4$:Mo	–	4750 μmol h^{-1} g^{-1}	Xenon Lamp $\lambda \geq 420$ nm	[122]
33	$Cd_{0.5}Zn_{0.5}S$/$BiVO_4$	–	2350 μmol h^{-1} g^{-1}	Xenon Lamp $\lambda \geq 420$ nm	[123]
34	BP/$BiVO_4$	–	160 μmol h^{-1} g^{-1}	$\lambda \geq 420$ nm	[124]
35	Bi_2MoO_6/g-C_3N_4	–	563.4 μmol h^{-1} g^{-1}	Xenon lamp $\lambda > 420$ nm	[126]
36	CQDs/Bi_2MoO_6	–	4.9 μmol h^{-1}	Xenon lamp	[127]
37	Bi_2O_3/Bi_2MoO_6	–	52 μmol g^{-1}	Xenon lamp $\lambda > 420$ nm	[128]
38	Bi_4NbO_8Cl/Nb_2O_5	–	169 μmol h^{-1}	Xenon lamp $\lambda > 300$ nm	[162]
39	BiOI	2.04 eV	1316.9 μmol g^{-1} h^{-1}	Xenon lamp $\lambda \geq 400$ nm	[38]

Please cite this article as: Saddique Z et al., Bismuth-based nanomaterials-assisted photocatalytic water splitting for sustainable hydrogen production, International Journal of Hydrogen Energy, https://doi.org/10.1016/j.ijhydene.2023.05.047

Table 1 – (*continued*)

Sr. No.	Bismuth-based materials	Band Gap	Hydrogen production	Light source	Ref.
Bismuth-based bulk compounds as a photocatalyst for hydrogen production					
40	$Bi_{24}O_{31}Br_{10}$	–	3.3 μmol h^{-1}	Xenon lamp λ > 400 nm	[129]
41	Bi_2WO_6	2.8 eV	1.6 μmol g^{-1} h^{-1}	Mercury lamp λ > 420 nm	[130]
42	BiOCl	–	0.12 μmol h^{-1}	Xenon lamp λ ≥ 420 nm	[95]
43	$Bi_2W_2O_9$	3.0 eV	18 μmol g^{-1} h^{-1}	Mercury lamp λ > 420 nm	[130]
44	$Bi_4Ti_3O_{12}$	3.1 eV	0.6 μmol g^{-1} h^{-1}	Mercury lamp λ > 420 nm	[130]
45	Bi_3TiNbO_9	3.1 eV	33 μmol g^{-1} h^{-1}	Mercury lamp λ > 420 nm	[130]
46	$BiMoO_6$	3.0 eV	0.01 μmol g^{-1} h^{-1}	Mercury lamp λ > 420 nm	[130]
47	$BaBi_4Ti_4O_{15}$	3.3 eV	8.2 μmol g^{-1} h^{-1}	Mercury lamp λ > 420 nm	[130]
48	$PbBi_2Nb_2O_9$	2.88 eV	7.6 μmol h^{-1}	Tungsten lamp λ ≥ 420 nm	[131]
49	$PbBi_2Nb_2O_9$	2.88 eV	3.2 μmol h^{-1}	Xenon lamp λ ≥ 420 nm	[132]
50	$PbBi_4Ti_4O_{15}$	3.02 eV	11.2 μmol h^{-1}	Xenon lamp λ ≥ 420 nm	[132]
51	Bi_4NbO_8Cl	2.39 eV	0.1 μmol h^{-1}	λ > 420	[86]
52	$BiYWO_6$	2.71 eV	4.1 μmol h^{-1}	Xenon lamp λ > 420	[97]
53	$Bi_2Ga_4O_9$	2.93 eV	19.3 μmol g^{-1} h^{-1}	Hg Lamp λ > 400 nm	[93]
54	$Bi_2Y_2NbO_8Cl$	–	113 μmol h^{-1}	Xenon lamp λ > 380 nm	[162]
55	$BiNb(Ta)O_4$:Cr	–	7 μmol g^{-1} h^{-1}	Xe–Hg Lamp λ > 418	[133]
Bismuth-based non-stoichiometric compounds as a photocatalyst for hydrogen production					
56	$Bi_2Ga_{3.6}Fe_{0.4}O_9$	2.2 eV	41.5 μmol g^{-1} h^{-1}	Hg Lamp λ > 400 nm	[93]
57	$Sr_{0.9}Bi_{0.1}Ti_{0.9}Fe_{0.1}O_3$	2.2 eV	180 μmol h^{-1}	Xenon lamp λ ≥ 250 nm	[135]
58	$Sr_{0.6}Bi_{0.4}Ti_{0.6}Fe_{0.4}O_3$	2.7 eV	50 μmol h^{-1}	Xenon lamp λ ≥ 250 nm	[136]
59	$(Na\ Bi)_{0.5}MoO_4$	3.1 eV	0.6 μmol h^{-1}	Xenon Lamp	[134]
60	$(Na\ Bi)_{0.5}WO_4$	3.5 eV	7.0 μmol h^{-1}	Xenon Lamp	[134]
61	$(Ag\ Bi)_{0.5}WO_4$	3.2 eV	0.1 μmol h^{-1}	Xenon Lamp	[134]
62	$Bi_{0.5}Na_{0.5}TiO_3$	2.92 eV	325.4 μmol g^{-1} h^{-1}	Xenon Lamp	[137]
63	$Na(Bi_{0.08}Ta_{0.92})O_3$	2.88 eV	59.48 μmol g^{-1} h^{-1}	Xenon Lamp λ > 400 nm	[139]
64	NiO_x-$Bi_4Ti_{2.6}Cr_{0.4}O_{12}$	2.42 eV	98 μmol h^{-1}	Xenon lamp λ > 400 nm	[141]
65	$Bi_4Ti_{2.6}Cr_{0.4}O_{12}$	2.42 eV	117 μmol g^{-1} h^{-1}	Xenon lamp λ > 420 nm	[140]
66	$Bi_{0.5}Dy_{0.5}VO_4$	2.76 eV	58.62 μmol h^{-1}	Xenon Lamp λ > 420 nm	[142,143]
67	$Bi_{0.5}Y_{0.5}VO_4$	3.02 eV	402 μmol h^{-1}	Mercury lamp λ > 300 nm	[144]
68	$Bi_{0.5}Sm_{0.5}VO_4$	3.06 eV	188.25 μmol g^{-1} h^{-1}	Xenon Lamp λ > 300 nm	[149]

Additionally, some photocatalysts require costly and noble co-catalysts to catalyze water splitting. Furthermore, an unsuitable band structure or band positions in a photocatalyst can lead to low efficiency or even complete inactivation. Regarding the photocatalytic mechanism, challenges include photo-corrosion, poor stability, limited light-harvesting capacity, and rapid electron-hole recombination, resulting in low energy efficiency and hindering industrial-scale upgradation of the process. Charge trapping and minimization of energy loss are two interrelated phenomena in photocatalysis. Energy loss occurs due to the recombination of photogenerated electron/hole pairs, which can be mitigated by the introduction of trap sites in the semiconductor photocatalyst. These trap sites are responsible for impeding charge

Please cite this article as: Saddique Z et al., Bismuth-based nanomaterials-assisted photocatalytic water splitting for sustainable hydrogen production, International Journal of Hydrogen Energy, https://doi.org/10.1016/j.ijhydene.2023.05.047

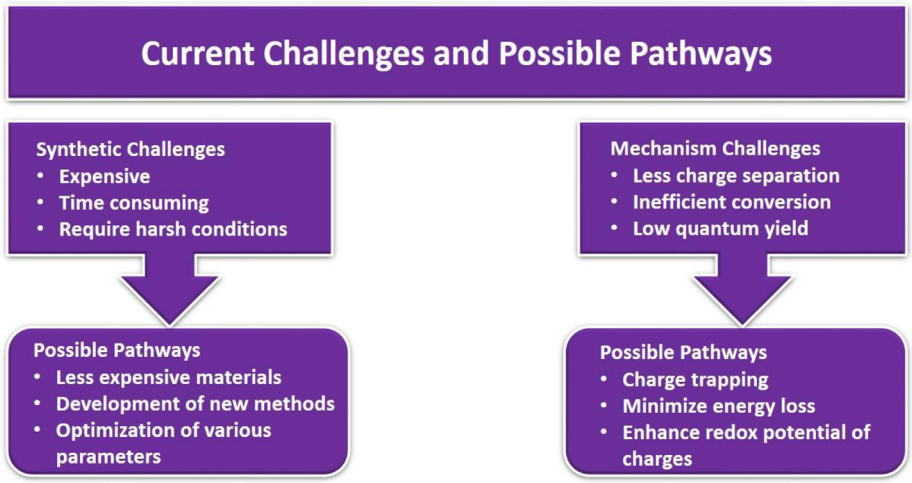

Fig. 11 – Current challenges and possible pathways for application of bismuth-based materials for photocatalytic water splitting.

recombination, which leads to the minimization of energy loss and an increase in hydrogen production. To achieve efficient and scalable hydrogen production through photocatalytic water splitting, there is a need to develop photocatalysts with suitable band structures and stability, as well as one-step photocatalytic water splitting processes. Band engineering and optimization of the photocatalytic mechanism should also be pursued to eliminate the need for expensive co-catalysts while maintaining high performance. Additionally, optimizing operating conditions such as pH and temperature is essential for scaling up hydrogen generation to meet the growing demand.

Conclusion

This article presents a comprehensive summary of recent literature on photocatalytic hydrogen production, discussing the energy demands that are leading to an impending energy crisis and the potential of hydrogen as a renewable and alternative fuel.

Based on recent reports, we elaborate on the synthesis of bismuth-based photocatalysts including nanomaterials, composites, bulk compounds and non-stoichiometric compounds, highlighting their promising efficiency for photocatalytic hydrogen production via several bismuth-based materials. The literature suggests that band structure is more critical factor than band gap for photocatalytic performance in hydrogen evolution. In addition, this review highlights the limitations in the field and suggests potential solutions. The technical information presented in this review is intended to provide guidance to experts in the field to advance photocatalytic hydrogen production and upscale to meet the global energy demands. It is hoped that this review will inspire further research to develop advanced photocatalysts with optimized photocatalytic mechanisms.

Declaration of competing interest

The authors declare that they have no known competing financial interests or personal relationships that could have appeared to influence the work reported in this paper.

REFERENCES

[1] Yao Y, et al. Photocatalytic reforming for hydrogen evolution: a review. Catalysts 2020;10(3):335.
[2] Davis KA, et al. Photocatalytic hydrogen evolution from biomass conversion. Nano Convergence 2021;8(1):1–19.
[3] Shi J, Guo L. ABO3-based photocatalysts for water splitting. Prog Nat Sci: Mater Int 2012;22(6):592–615.
[4] Joy J, Mathew J, George SC. Nanomaterials for photoelectrochemical water splitting–review. Int J Hydrogen Energy 2018;43(10):4804–17.
[5] Ahmad H, et al. Hydrogen from photo-catalytic water splitting process: a review. Renew Sustain Energy Rev 2015;43:599–610.
[6] Walter MG, et al. Solar water splitting cells. Chem Rev 2010;110(11):6446–73.
[7] Lewis NS, Nocera DG. Powering the planet: chemical challenges in solar energy utilization. Proc Natl Acad Sci USA 2006;103(43):15729–35.
[8] Lewis NS, Crabtree G, Nozik AJ, Wasielewski MR, Alivisatos P, Kung H, et al. Basic research needs for solar energy utilization. report of the basic energy sciences workshop on solar energy utilization. DOESC (USDOE Office of Science (SC)) 2005. April 18-21, 2005.
[9] Fujishima A, Honda K. Electrochemical photolysis of water at a semiconductor electrode. Nature 1972;238(5358):37–8.
[10] Linsebigler AL, Lu G, Yates Jr JT. Photocatalysis on TiO2 surfaces: principles, mechanisms, and selected results. Chem Rev 1995;95(3):735–58.
[11] Zou Z, et al. Direct splitting of water under visible light irradiation with an oxide semiconductor photocatalyst. Nature 2001;414(6864):625–7.

Please cite this article as: Saddique Z et al., Bismuth-based nanomaterials-assisted photocatalytic water splitting for sustainable hydrogen production, International Journal of Hydrogen Energy, https://doi.org/10.1016/j.ijhydene.2023.05.047

[12] Ran J, et al. Earth-abundant cocatalysts for semiconductor-based photocatalytic water splitting. Chem Soc Rev 2014;43(22):7787–812.
[13] Wei Z, et al. Photocatalytic hydrogen evolution with simultaneous antibiotic wastewater degradation via the visible-light-responsive bismuth spheres-g-C3N4 nanohybrid: waste to energy insight. Chem Eng J 2019;358:944–54.
[14] Chen W-T, et al. Effect of TiO2 polymorph and alcohol sacrificial agent on the activity of Au/TiO2 photocatalysts for H2 production in alcohol–water mixtures. J Catal 2015;329:499–513.
[15] Chen X, et al. Semiconductor-based photocatalytic hydrogen generation. Chem Rev 2010;110(11):6503–70.
[16] Acar C, Dincer I, Naterer GF. Review of photocatalytic water-splitting methods for sustainable hydrogen production. Int J Energy Res 2016;40(11):1449–73.
[17] Osterloh FE, Parkinson BA. Recent developments in solar water-splitting photocatalysis. MRS Bull 2011;36(1):17–22.
[18] Yang Y, et al. Progress in developing metal oxide nanomaterials for photoelectrochemical water splitting. Adv Energy Mater 2017;7(19):1700555.
[19] Liu Y, et al. Bismuth-based complex oxides for photocatalytic applications in environmental remediation and water splitting: a review. Sci Total Environ 2022;804:150215.
[20] Ke J, et al. Facile assembly of Bi2O3/Bi2S3/MoS2 np heterojunction with layered n-Bi2O3 and p-MoS2 for enhanced photocatalytic water oxidation and pollutant degradation. Appl Catal B Environ 2017;200:47–55.
[21] Monny SA, et al. Bismuth based photoelectrodes for solar water splitting. J Energy Chem 2021;61:517–30.
[22] Reber JF, Meier K. Photochemical production of hydrogen with zinc sulfide suspensions. J Phys Chem 1984;88(24):5903–13.
[23] Liang J, et al. A review on gC 3 N 4 incorporated with organics for enhanced photocatalytic water splitting. J Mater Chem 2021;9(22):12898–922.
[24] Wang Y, Wang X, Antonietti M. Polymeric graphitic carbon nitride as a heterogeneous organocatalyst: from photochemistry to multipurpose catalysis to sustainable chemistry. Angew Chem Int Ed 2012;51(1):68–89.
[25] Yi Z, et al. An orthophosphate semiconductor with photooxidation properties under visible-light irradiation. Nat Mater 2010;9(7):559–64.
[26] Xu X, et al. A red metallic oxide photocatalyst. Nat Mater 2012;11(7):595–8.
[27] Tao X, et al. Bismuth tantalum oxyhalogen: a promising candidate photocatalyst for solar water splitting. Adv Energy Mater 2018;8(1):1701392.
[28] Zhang J, et al. Preparation of ZnS/CdS composite nanoparticles by coprecipitation from reverse micelles using CO2 as antisolvent. J Colloid Interface Sci 2004;273(1):160–4.
[29] Innocenti M, et al. Ternary cadmium and zinc sulfides: composition, morphology and photoelectrochemistry. Electrochim Acta 2004;49(8):1327–37.
[30] Yan H, et al. Visible-light-driven hydrogen production with extremely high quantum efficiency on Pt–PdS/CdS photocatalyst. J Catal 2009;266(2):165–8.
[31] Hlophe PV, Dlamini LN. Synthesis of a semi-conductor-like MOF with black phosphorous as a composite for visible light-driven photocatalysis. RSC Adv 2019;9(64):37321–30.
[32] Sun S, et al. Engineering interfacial band bending over bismuth vanadate/carbon nitride by work function regulation for efficient solar-driven water splitting. Sci Bull 2022;67(4):389–97.
[33] Chen X, et al. Increasing solar absorption for photocatalysis with black hydrogenated titanium dioxide nanocrystals. Science 2011;331(6018):746–50.
[34] Zhou X, et al. Controlled synthesis of CdS nanoparticles and their surface loading with MoS2 for hydrogen evolution under visible light. Int J Hydrogen Energy 2016;41(33):14758–67.
[35] Puangpetch T, et al. Hydrogen production from photocatalytic water splitting over mesoporous-assembled SrTiO3 nanocrystal-based photocatalysts. J Mol Catal Chem 2009;312(1–2):97–106.
[36] Li X, et al. Au Multimer@ MoS2 hybrid structures for efficient photocatalytical hydrogen production via strongly plasmonic coupling effect. Nano Energy 2016;30:549–58.
[37] Ding C, et al. Large-scale preparation of BiOX (X= Cl, Br) ultrathin nanosheets for efficient photocatalytic CO2 conversion. J Taiwan Inst Chem Eng 2017;78:395–400.
[38] Lee G-J, Zheng Y-C, Wu JJ. Fabrication of hierarchical bismuth oxyhalides (BiOX, X= Cl, Br, I) materials and application of photocatalytic hydrogen production from water splitting. Catal Today 2018;307:197–204.
[39] Dong X-D, Zhang Y-M, Zhao Z-Y. Role of the polar electric field in bismuth oxyhalides for photocatalytic water splitting. Inorg Chem 2021;60(12):8461–74.
[40] Ansari K, et al. Nanoporous carbon doped ceria bismuth oxide solid solution for photocatalytic water splitting. Sustain Energy Fuels 2021;5(9):2545–62.
[41] Kudo A, Miseki Y. Heterogeneous photocatalyst materials for water splitting. Chem Soc Rev 2009;38(1):253–78.
[42] Jing D, et al. Efficient solar hydrogen production by photocatalytic water splitting: from fundamental study to pilot demonstration. Int J Hydrogen Energy 2010;35(13):7087–97.
[43] Chen WH, et al. A review on the visible light active modified photocatalysts for water splitting for hydrogen production. Int J Energy Res 2022;46(5):5467–77.
[44] Zhu Z, et al. Recent advances in bismuth-based multimetal oxide photocatalysts for hydrogen production from water splitting: competitiveness, challenges, and future perspectives. Materials Reports: Energy 2021;1(2):100019.
[45] Bhat SS, Jang HW. Recent advances in bismuth-based nanomaterials for photoelectrochemical water splitting. ChemSusChem 2017;10(15):3001–18.
[46] Tian N, et al. Layered bismuth-based photocatalysts. Coord Chem Rev 2022;463:214515.
[47] Stanley JC, Mayr F, Gagliardi A. Machine learning stability and bandgaps of lead-free perovskites for photovoltaics. Advanced Theory and Simulations 2020;3(1):1900178.
[48] Corti M, et al. Application of metal halide perovskites as photocatalysts in organic reactions. INORGA 2021;9(7):56.
[49] Dong Q, et al. Electron-hole diffusion lengths> 175 μm in solution-grown CH3NH3PbI3 single crystals. Science 2015;347(6225):967–70.
[50] Xing G, et al. Long-range balanced electron-and hole-transport lengths in organic-inorganic CH3NH3PbI3. Science 2013;342(6156):344–7.
[51] Chen Q, et al. Under the spotlight: The organic–inorganic hybrid halide perovskite for optoelectronic applications. Nano Today 2015;10(3):355–96.
[52] Ji Y, et al. In-depth Understanding of the Effect of halogen-induced stable 2D bismuth-based Perovskites for photocatalytic hydrogen evolution activity. Adv Funct Mater 2022;32(31):2201721.
[53] Wu Z, et al. Recent developments in lead-free bismuth-based halide perovskite nanomaterials for heterogeneous photocatalysis under visible light. Nanoscale 2023;15:5598–622.
[54] Tedesco C, Malavasi L. Bismuth-based halide Perovskites for photocatalytic H2 evolution application. Molecules 2023;28(1):339.
[55] Bresolin B-M, et al. Cs3Bi2I9/g-C3N4 as a new binary photocatalyst for efficient visible-light photocatalytic processes. Sep Purif Technol 2020;251:117320.

Please cite this article as: Saddique Z et al., Bismuth-based nanomaterials-assisted photocatalytic water splitting for sustainable hydrogen production, International Journal of Hydrogen Energy, https://doi.org/10.1016/j.ijhydene.2023.05.047

[56] Malavasi L, Tedesco C. Bismuth-based halide perovskites for photocatalytic H2 evolution application. 2022.
[57] Zhang Y, et al. Combinatorial substrate epitaxy: a high-throughput method for determining phase and orientation relationships and its application to BiFeO3/TiO2 heterostructures. Acta Mater 2012;60(19):6486–93.
[58] Thalluri SM, et al. Green-synthesized W-and Mo-doped BiVO4 oriented along the {0 4 0} facet with enhanced activity for the sun-driven water oxidation. Appl Catal B Environ 2016;180:630–6.
[59] Hassanzadeh-Afruzi F. Synergistic photocatalytic effect. In: Heterogeneous micro and nanoscale composites for the catalysis of organic reactions. Elsevier; 2022. p. 183–95.
[60] Maeda K, Domen K. Photocatalytic water splitting: recent progress and future challenges. J Phys Chem Lett 2010;1(18):2655–61.
[61] Lede J, Lapicque F, Villermaux J. Production of hydrogen by direct thermal decomposition of water. Int J Hydrogen Energy 1983;8(9):675–9.
[62] Cecal A, et al. Radiolytic splitting of water molecules in the presence of some supramolecular compounds. J Serb Chem Soc 2003;68(7):593–8.
[63] Akkerman I, et al. Photobiological hydrogen production: photochemical efficiency and bioreactor design. Int J Hydrogen Energy 2002;27(11–12):1195–208.
[64] Dincer I, Acar C. Review and evaluation of hydrogen production methods for better sustainability. Int J Hydrogen Energy 2015;40(34):11094–111.
[65] Yerga R, et al. Chem-SusChem: chem. Sustain. Energy Mater 2009;2:471–85.
[66] Takata T, Domen K. Particulate photocatalysts for water splitting: recent advances and future prospects. ACS Energy Lett 2019;4(2):542–9.
[67] Bard AJ. Photoelectrochemistry and heterogeneous photocatalysis at semiconductors. J Photochem 1979;10(1):59–75.
[68] Wang Q, Domen K. Particulate photocatalysts for light-driven water splitting: mechanisms, challenges, and design strategies. Chem Rev 2019;120(2):919–85.
[69] Lee Y, et al. Zinc germanium oxynitride as a photocatalyst for overall water splitting under visible light. J Phys Chem C 2007;111(2):1042–8.
[70] Maeda K, et al. GaN: ZnO solid solution as a photocatalyst for visible-light-driven overall water splitting. J Am Chem Soc 2005;127(23):8286–7.
[71] Sayama K, et al. Stoichiometric water splitting into H2 and O2 using a mixture of two different photocatalysts and an IO3−/I− shuttle redox mediator under visible light irradiation. Chem Commun 2001;(23):2416–7.
[72] Kato H, et al. Construction of Z-scheme type heterogeneous photocatalysis systems for water splitting into H2 and O2 under visible light irradiation. Chem Lett 2004;33(10):1348–9.
[73] Qi Y, et al. Unraveling of cocatalysts photodeposited selectively on facets of BiVO4 to boost solar water splitting. Nat Commun 2022;13(1):1–9.
[74] Yang Y, Kang L, Li H. Enhancement of photocatalytic hydrogen production of BiFeO3 by Gd3+ doping. Ceram Int 2019;45(6):8017–22.
[75] Yuan L, et al. Photocatalytic water splitting for solar hydrogen generation: fundamentals and recent advancements. Int Rev Phys Chem 2016;35(1):1–36.
[76] Tong H, et al. Nano-photocatalytic materials: possibilities and challenges. Adv Mater 2012;24(2):229–51.
[77] Makuła P, Pacia M, Macyk W. How to correctly determine the band gap energy of modified semiconductor photocatalysts based on UV–Vis spectra. ACS Publications 2018:6814–7.
[78] Bolts JM, Wrighton MS. Correlation of photocurrent-voltage curves with flat-band potential for stable photoelectrodes for the photoelectrolysis of water. J Phys Chem 1976;80(24):2641–5.
[79] Zhou Z. Journal of Materials Chemistry A and Materials Advances Editor's choice web collection:"Machine learning for materials innovation". J Mater Chem 2021;9(3):1295–6.
[80] Su T, et al. Role of interfaces in two-dimensional photocatalyst for water splitting. ACS Catal 2018;8(3):2253–76.
[81] Rafique M, et al. A comprehensive study on methods and materials for photocatalytic water splitting and hydrogen production as a renewable energy resource. J Inorg Organomet Polym Mater 2020;30(10):3837–61.
[82] Rafique M, et al. Investigation of photocatalytic and seed germination effects of TiO2 nanoparticles synthesized by Melia azedarach L. leaf extract. J Inorg Organomet Polym Mater 2019;29(6):2133–44.
[83] Tentu RD, Basu S. Photocatalytic water splitting for hydrogen production. Current Opinion in Electrochemistry 2017;5(1):56–62.
[84] Meng X, Zhang Z. Bismuth-based photocatalytic semiconductors: introduction, challenges and possible approaches. J Mol Catal Chem 2016;423:533–49.
[85] Ghosh I, et al. Organic semiconductor photocatalyst can bifunctionalize arenes and heteroarenes. Science 2019;365(6451):360–6.
[86] Fujito H, et al. Layered perovskite oxychloride Bi4NbO8Cl: a stable visible light responsive photocatalyst for water splitting. J Am Chem Soc 2016;138(7):2082–5.
[87] Tahir MB, et al. Functionalized role of highly porous activated carbon in bismuth vanadate nanomaterials for boosted photocatalytic hydrogen evolution and synchronous activity in water. Int J Hydrogen Energy 2021;46(80):39778–85.
[88] Huizhong A, et al. Photocatalytic properties of biox (X= Cl, Br, and I). Rare Met 2008;27(3):243–50.
[89] Meng X, Zhang Z. Facile synthesis of BiOBr/Bi2WO6 heterojunction semiconductors with high visible-light-driven photocatalytic activity. J Photochem Photobiol Chem 2015;310:33–44.
[90] Ogawa K, et al. Layered perovskite oxyiodide with narrow band gap and long lifetime carriers for water splitting photocatalysis. J Am Chem Soc 2021;143(22):8446–53.
[91] Kuriki R, et al. A stable, narrow-gap oxyfluoride photocatalyst for visible-light hydrogen evolution and carbon dioxide reduction. J Am Chem Soc 2018;140(21):6648–55.
[92] Li J, Yu Y, Zhang L. Bismuth oxyhalide nanomaterials: layered structures meet photocatalysis. Nanoscale 2014;6(15):8473–88.
[93] Yang J, et al. Bi2Ga4O9: An undoped single-phase photocatalyst for overall water splitting under visible light. J Catal 2017;345:236–44.
[94] Han L, et al. Efficient water-splitting device based on a bismuth vanadate photoanode and thin-film silicon solar cells. ChemSusChem 2014;7(10):2832–8.
[95] Ye L, et al. Synthesis of black ultrathin BiOCl nanosheets for efficient photocatalytic H2 production under visible light irradiation. J Power Sources 2015;293:409–15.
[96] Wang L, et al. Visible light responsive bismuth niobate photocatalyst: enhanced contaminant degradation and hydrogen generation. J Mater Chem 2010;20(38):8405–10.
[97] Liu H, et al. Visible-light-responding BiYWO6 solid solution for stoichiometric photocatalytic water splitting. J Phys Chem C 2008;112(23):8521–3.
[98] Nagabhushana G, Nagaraju G, Chandrappa G. Synthesis of bismuth vanadate: its application in H 2 evolution and sunlight-driven photodegradation. J Mater Chem 2013;1(2):388–94.

Please cite this article as: Saddique Z et al., Bismuth-based nanomaterials-assisted photocatalytic water splitting for sustainable hydrogen production, International Journal of Hydrogen Energy, https://doi.org/10.1016/j.ijhydene.2023.05.047

[99] Sun S, et al. Solar light driven pure water splitting on quantum sized BiVO4 without any cocatalyst. ACS Catal 2014;4(10):3498–503.
[100] Zhou Y, et al. Monolayered Bi2WO6 nanosheets mimicking heterojunction interface with open surfaces for photocatalysis. Nat Commun 2015;6(1):1–8.
[101] Panmand RP, et al. Self-assembled hierarchical nanostructures of Bi 2 WO 6 for hydrogen production and dye degradation under solar light. CrystEngComm 2015;17(1):107–15.
[102] Li J, et al. Facet-level mechanistic Insights into general homogeneous carbon Doping for enhanced solar-to-hydrogen conversion. Adv Funct Mater 2015;25(14):2189–201.
[103] Zhang L, et al. Solar-light-driven pure water splitting with ultrathin BiOCl nanosheets. Chem–Eur J 2015;21(50):18089–94.
[104] Murugesan S, Subramanian VR. Robust synthesis of bismuth titanate pyrochlore nanorods and their photocatalytic applications. Chem Commun 2009;(34):5109–11.
[105] Su Y, Zhang L, Wang W. Internal polar field enhanced H2 evolution of BiOIO3 nanoplates. Int J Hydrogen Energy 2016;41(24):10170–7.
[106] Zhang L, et al. Water splitting from dye wastewater: a case study of BiOCl/copper (II) phthalocyanine composite photocatalyst. Appl Catal B Environ 2013;132:315–20.
[107] Zhang L, et al. Selective transport of electron and hole among {0 0 1} and {1 1 0} facets of BiOCl for pure water splitting. Appl Catal B Environ 2015;162:470–4.
[108] Al-Namshah KS, Mohamed RM. Nd-doped Bi2O3 nanocomposites: simple synthesis and improved photocatalytic activity for hydrogen production under visible light. Appl Nanosci 2018;8(5):1233–9.
[109] Li J, et al. Superior visible light hydrogen evolution of Janus bilayer junctions via atomic-level charge flow steering. Nat Commun 2016;7(1):1–9.
[110] Chen D, Tang L, Li J. Graphene-based materials in electrochemistry. Chem Soc Rev 2010;39(8):3157–80.
[111] Pan B, et al. Nanocomposite of BiPO4 and reduced graphene oxide as an efficient photocatalyst for hydrogen evolution. Int J Hydrogen Energy 2014;39(25):13527–33.
[112] Zhao J, et al. Bi2MoO6/RGO composite nanofibers: facile electrospinning fabrication, structure, and significantly improved photocatalytic water splitting activity. J Mater Sci Mater Electron 2017;28(1):543–52.
[113] Sun Z, et al. A high-performance Bi 2 WO 6–graphene photocatalyst for visible light-induced H 2 and O 2 generation. Nanoscale 2014;6(4):2186–93.
[114] Hu J, et al. Z-Scheme 2D/2D heterojunction of black phosphorus/monolayer Bi2WO6 nanosheets with enhanced photocatalytic activities. Angew Chem Int Ed 2019;58(7):2073–7.
[115] Sun F, et al. Flexible self-supporting bifunctional [TiO2/C]//[Bi2WO6/C] carbon-based Janus nanofiber heterojunction photocatalysts for efficient hydrogen evolution and degradation of organic pollutant. J Alloys Compd 2020;830:154673.
[116] Qiang Z, et al. Iodine doped Z-scheme Bi2O2CO3/Bi2WO6 photocatalysts: facile synthesis, efficient visible light photocatalysis, and photocatalytic mechanism. Chem Eng J 2021;403:126327.
[117] Arif M, et al. A Bi2WO6-based hybrid heterostructures photocatalyst with enhanced photodecomposition and photocatalytic hydrogen evolution through Z-scheme process. J Ind Eng Chem 2019;69:345–57.
[118] Chang C-J, et al. Enhanced photocatalytic H2 production activity of Ag-doped Bi2WO6-graphene based photocatalysts. Int J Hydrogen Energy 2018;43(24):11345–54.
[119] Wu S, et al. Effects of surface terminations of 2D Bi2WO6 on photocatalytic hydrogen evolution from water splitting. ACS Appl Mater Interfaces 2020;12(17):20067–74.
[120] Hu J, et al. Spatially separating redox centers on Z-scheme ZnIn2S4/BiVO4 hierarchical heterostructure for highly efficient photocatalytic hydrogen evolution. Small 2020;16(37):2002988.
[121] Fu Y, et al. All-solid-state Z-scheme system of NiO/CDs/BiVO4 for visible light-driven efficient overall water splitting. Chem Eng J 2019;358:134–42.
[122] Wang Q, et al. Scalable water splitting on particulate photocatalyst sheets with a solar-to-hydrogen energy conversion efficiency exceeding 1%. Nat Mater 2016;15(6):611–5.
[123] Zeng C, et al. A core–satellite structured Z-scheme catalyst Cd 0.5 Zn 0.5 S/BiVO 4 for highly efficient and stable photocatalytic water splitting. J Mater Chem 2018;6(35):16932–42.
[124] Zhu M, et al. Z-scheme photocatalytic water splitting on a 2D heterostructure of black phosphorus/bismuth vanadate using visible light. Angew Chem Int Ed 2018;57(8):2160–4.
[125] Ma Y, et al. A simple process to prepare few-layer g-C3N4 nanosheets with enhanced photocatalytic activities. Appl Surf Sci 2015;358:246–51.
[126] Li J, et al. In situ growing Bi2MoO6 on g-C3N4 nanosheets with enhanced photocatalytic hydrogen evolution and disinfection of bacteria under visible light irradiation. J Hazard Mater 2017;321:183–92.
[127] Zhang Z, et al. Carbon quantum dots/Bi2MoO6 composites with photocatalytic H2 evolution and near infrared activity. J Photochem Photobiol Chem 2017;346:24–31.
[128] Fu F, et al. Alkali-assisted synthesis of direct Z-scheme based Bi2O3/Bi2MoO6 photocatalyst for highly efficient photocatalytic degradation of phenol and hydrogen evolution reaction. J Catal 2019;375:399–409.
[129] Shang J, et al. Bismuth oxybromide with reasonable photocatalytic reduction activity under visible light. ACS Catal 2014;4(3):954–61.
[130] Kudo A, Hijii S. H2 or O2 evolution from aqueous solutions on layered oxide photocatalysts consisting of Bi3+ with 6s2 configuration and d0 transition metal ions. Chem Lett 1999;28(10):1103–4.
[131] Kim HG, Hwang DW, Lee JS. An undoped, single-phase oxide photocatalyst working under visible light. J Am Chem Soc 2004;126(29):8912–3.
[132] Kim HG, et al. A generic method of visible light sensitization for perovskite-related layered oxides: Substitution effect of lead. J Solid State Chem 2006;179(4):1214–8.
[133] Almeida CG, et al. Photocatalytic hydrogen production with visible light over Mo and Cr-doped BiNb (Ta) O4. Int J Hydrogen Energy 2014;39(3):1220–7.
[134] Kato H, Matsudo N, Kudo A. Photophysical and photocatalytic properties of molybdates and tungstates with a scheelite structure. Chem Lett 2004;33(9):1216–7.
[135] Lu L, et al. Photocatalytic hydrogen production over solid solutions between BiFeO3 and SrTiO3. Appl Surf Sci 2017;391:535–41.
[136] Lu L, et al. Efficient photocatalytic hydrogen production over solid solutions Sr1-xBixTi1-xFexO3 (0≤ x≤ 0.5). Appl Catal B Environ 2017;200:412–9.
[137] Wang L, Wang W. Photocatalytic hydrogen production from aqueous solutions over novel Bi0. 5Na0. 5TiO3 microspheres. Int J Hydrogen Energy 2012;37(4):3041–7.
[138] Kanhere P, Zheng J, Chen Z. Visible light driven photocatalytic hydrogen evolution and photophysical properties of Bi3+ doped NaTaO3. Int J Hydrogen Energy 2012;37(6):4889–96.

Please cite this article as: Saddique Z et al., Bismuth-based nanomaterials-assisted photocatalytic water splitting for sustainable hydrogen production, International Journal of Hydrogen Energy, https://doi.org/10.1016/j.ijhydene.2023.05.047

[139] Li Z, et al. Photocatalytic hydrogen production from aqueous methanol solutions under visible light over Na (BixTa1−x) O3 solid-solution. Int J Hydrogen Energy 2009;34(1):147−52.
[140] Chen Z, et al. Chromium-modified Bi4Ti3O12 photocatalyst: application for hydrogen evolution and pollutant degradation. Appl Catal B Environ 2016;199:241−51.
[141] Hou J, et al. Chromium-doped bismuth titanate nanosheets as enhanced visible-light photocatalysts with a high percentage of reactive {110} facets. J Mater Chem 2011;21(20):7296−301.
[142] Wang Q, et al. Visible-light-responding Bi0. 5Dy0. 5VO4 solid solution for photocatalytic water splitting. Catal Lett 2009;131(1):160−3.
[143] Wang Q, et al. Photocatalytic water splitting by band-gap engineering of solid solution Bi1− xDyxVO4 and Bi0. 5M0. 5VO4 (M= La, Sm, Nd, Gd, Eu, Y). J Alloys Compd 2012;522:19−24.
[144] Liu H, et al. Novel photocatalyst of V-based solid solutions for overall water splitting. J Mater Chem 2011;21(41):16535−43.
[145] Liu H, et al. Roles of Bi, M and VO4 tetrahedron in photocatalytic properties of novel Bi0. 5M0. 5VO4 (M= La, Eu, Sm and Y) solid solutions for overall water splitting. J Solid State Chem 2012;186:70−5.
[146] Fang W, et al. Effect of surface self-heterojunction existed in Bi x Y1−x VO4 on photocatalytic overall water splitting. ACS Sustainable Chem Eng 2017;5(8):6578−84.
[147] Yu L, et al. BixY1− xVO4 solid solution with porous surface synthesized by molten salt method for photocatalytic water splitting. Int J Hydrogen Energy 2017;42(10):6519−25.
[148] Fang W, et al. Novel dodecahedron BiVO4: YVO4 solid solution with enhanced charge separation on adjacent exposed facets for highly efficient overall water splitting. J Catal 2017;352:155−9.
[149] Wang Q, et al. Photocatalytic water splitting into hydrogen and research on synergistic of Bi/Sm with solid solution of Bi−Sm−V photocatalyst. Int J Hydrogen Energy 2012;37(17):12886−92.
[150] Ouedraogo S, et al. Bismuth oxybromide/reduced graphene oxide heterostructure sensitized with Zn-tetracarboxyphthalocyanine as a highly efficient photocatalyst for the degradation of Orange II and phenol. J Environ Chem Eng 2022;10(2):107332.
[151] Yang D, et al. NIR-driven water splitting by layered bismuth oxyhalide sheets for effective photodynamic therapy. J Mater Chem B 2017;5(22):4152−61.
[152] Ye K-H, et al. Carbon quantum dots as a visible light sensitizer to significantly increase the solar water splitting performance of bismuth vanadate photoanodes. Energy Environ Sci 2017;10(3):772−9.
[153] Abdi FF, et al. Efficient solar water splitting by enhanced charge separation in a bismuth vanadate-silicon tandem photoelectrode. Nat Commun 2013;4(1):1−7.
[154] Lee WC, et al. Copper-doped flower-like molybdenum disulfide/bismuth sulfide photocatalysts for enhanced solar water splitting. Int J Hydrogen Energy 2018;43(2):748−56.
[155] Chi J, et al. Recent advancements in bismuth vanadate photoanodes for photoelectrochemical water splitting. Mater Today Chem 2022;26:101060.
[156] Zhang K-L, et al. Study of the electronic structure and photocatalytic activity of the BiOCl photocatalyst. Appl Catal B Environ 2006;68(3−4):125−9.
[157] Kobayashi R, et al. A heterojunction photocatalyst composed of zinc rhodium oxide, single crystal-derived bismuth vanadium oxide, and silver for overall pure-water splitting under visible light up to 740 nm. Phys Chem Chem Phys 2016;18(40):27754−60.
[158] Kroeze JE, Savenije TJ, Warman JM. Electrodeless determination of the trap density, decay kinetics, and charge separation efficiency of dye-sensitized nanocrystalline TiO2. J Am Chem Soc 2004;126(24):7608−18.
[159] Rahman MZ, Kibria MG, Mullins CB. Metal-free photocatalysts for hydrogen evolution. Chem Soc Rev 2020;49(6):1887−931.
[160] Bisquert J. Interpretation of electron diffusion coefficient in organic and inorganic semiconductors with broad distributions of states. Phys Chem Chem Phys 2008;10(22):3175−94.
[161] Shen M, Henderson MA. Identification of the active species in photochemical hole scavenging reactions of methanol on TiO2. J Phys Chem Lett 2011;2(21):2707−10.
[162] Wei Z, et al. Enhanced photocatalytic hydrogen evolution using a novel in situ heterojunction yttrium-doped Bi4NbO8Cl@ Nb2O5. Int J Hydrogen Energy 2018;43(31):14281−92.

Please cite this article as: Saddique Z et al., Bismuth-based nanomaterials-assisted photocatalytic water splitting for sustainable hydrogen production, International Journal of Hydrogen Energy, https://doi.org/10.1016/j.ijhydene.2023.05.047